Interactive ocean bathymetry and coastlines for simulating the last deglaciation with the Max Planck Institute Earth System Model (MPI-ESM-v1.2)

Virna Loana Meccia[1] and Uwe Mikolajewicz[1]

[1]Max Planck Institute for Meteorology, Bundesstraße 53, 20146 Hamburg, Germany

Correspondence to: Virna Loana Meccia (virna.meccia@mpimet.mpg.de)

Abstract. As ice sheets grow or decay, the net flux of freshwater into the ocean changes and the bedrock adjusts due to isostatic adjustments, leading to variations in the bottom topography and the oceanic boundaries. This process was particularly intense during the last deglaciation due to the high rates of ice-sheet melting. It is, therefore, necessary to consider transient ocean bathymetry and coastlines when attempting to simulate the last deglaciation with Earth System Models (ESMs). However, in most standard ESMs the land-sea mask is fixed throughout simulations because the generation of a new ocean model bathymetry implies several levels of manual corrections, a procedure that is hardly doable very often for long runs. This is one of the main technical problems towards simulating a complete glacial cycle with general circulation models.

For the first time, we present a tool allowing for an automatic computation of bathymetry and land-sea mask changes in the Max Planck Institute Earth System Model (MPI-ESM). The algorithms developed in this paper can easily be adapted to any free-surface ocean model that uses Arakawa-C grid in the horizontal and z-grid in the vertical including partial bottom cells. The strategy applied is described in detail and the algorithms are tested in a long-term simulation demonstrating the reliable behaviour. Our approach guarantees the conservation of mass and tracers at global and regional scales, that is, changes in a single grid point are only propagated regionally. The procedures presented here are a brick stone in the development of a fully coupled ice sheet-solid earth-climate model system with time-varying topography and will ~~modules presented in this paper are a promising tool to be used with the MPI-ESM to~~ allow for transient simulations of the last deglaciation considering interactive bathymetry and land-sea mask.

1 Introduction

During the last deglaciation ~~Studying the climate of the past is essential to better understand the present climate and predict the changes in coming years or decades. The last deglaciation is of particular interest because it is a period of major climate change. During it~~, the Earth transitioned from the last glacial to the present interglacial climate, experiencing a series of abrupt changes on decadal to millennium timescales. The culmination of the last glacial cycle is denoted by the Last Glacial Maximum (LGM; ca. 21 thousand years before present (ka BP)) characterized by large ice sheets, cold oceans and low

greenhouse gas concentrations (Braconnot et al., 2007a; 2007b). During the LGM, vast ice sheets covered large regions of the Northern Hemisphere (e.g. Boulton et al., 2001; Dyke et al., 2002; Svendsen et al., 2004; Tarasov et al., 2012; Peltier et al., 2015), whereas the Antarctic Ice Sheet expanded to the edge of the continental shelf (Argus et al., 2014; Briggs et al., 2014; Lambeck et al., 2014 and references therein). The global annual mean surface temperature is estimated to have been 4.0 ± 0.8 degrees colder than today (Annan and Hargreaves, 2013); it started to increase towards the present value around 19 ka BP (Jouzel et al., 2007; Buizert et al., 2014). The reason of such a rise is attributed to an increase in the summer insolation at the northern hemisphere high latitudes and in the global atmospheric greenhouse gas concentrations (Berger, 1978; Loulergue et al., 2008; Marcott et al., 2014; Bereiter et al., 2015).

Nowadays, some complex Earth System Models (ESMs) can be run for multiple millennia becoming powerful tools for investigating the mechanisms underlying these climate change events. Especially, transient simulations of the last deglaciation might be valuable for examining the behaviour of non-stationary climate systems and the ice-ocean-atmosphere interactions. Since 1990's, the Paleoclimate Modeling Intercomparison Project (PMIP) aims at evaluating the performance of state-of-the-art climate models in simulating well-documented climates outside the range of present variability (Kageyama et al., 2018). Recently, PMIP has established the Last Deglaciation Working Group to coordinate the efforts to run transient simulations of the last 21 ka BP (Ivanovic et al., 2016). According to the authors, one aspect to be considered is the varying orography, ocean bathymetry, and land-sea mask. This is because changes in the ice sheets during the deglaciation affected continental topography and ocean bathymetry, which in turn moved the coastal boundaries. Differences in ocean bathymetry and land-sea mask between present-day conditions and 21 ka BP calculated from the ICE-6G_C ice-sheets reconstructions (Argus et al., 2014; Peltier et al., 2015) are plotted in Fig. 1. In general, the topography of the NH ice sheets does not vary substantially between different reconstructions whereas uncertainties show larger for Antarctica (Abe-Ouchi et al., 2015). Values up to 125 meters in ocean depth variations (Fig. 1a) are estimated, representing deepening of the ocean with time. The largest changes in the oceanic boundaries occurred in the northern hemisphere where the extensive areas covered by ice sheets during the LGM were flooded due to the ice melting (blue areas in Fig. 1b). It is important, therefore, to consider these changes when attempting to simulate the last deglaciation, for example by including a varying ocean surface area and volume.

There are many examples in the literature of the use of climate models to study the last deglaciation. Some works focus on the timing of the deglaciation (Liu et al., 2009; Menviel et al., 2011; Roche et al., 2011) and other studies address a particular component of the climate system. Many authors have investigated the effects of the glacial forcing on the atmosphere (Justino et al., 2005; Pausata et al., 2011; Otto-Bliesner et al., 2014) or on the ocean thermohaline circulation (Kim, 2004; Brady et al., 2013; Klockmann et al., 2016). Moreover, some research was carried out by using comprehensive climate and ice-sheet models (Abe-Ouchi et al, 2013) or ~~transient simulations with~~ climate models interactively coupled with a dynamic ice-sheet model for studying the last glacial-interglacial cycles (Bonelli et al., 2009; Heinemann et al., 2014; Ganopolski et al., 2016) and more specifically, the LGM (Ziemen et al., 2014). Still, in standard ESMs, land-sea mask is traditionally

treated as fixed. There are studies that consider a time-varying orography in coupled atmosphere-ocean-ice sheet models (e.g. Ridley et al., 2005, Mikolajewicz et al., 2007a and 2007b, Ziemen et al., 2014) but an interactive ocean bathymetry and coastlines for an ocean model have not been done yet. Liu et al. (2009) performed a transient simulation with the NCAR CCSM3 and they updated the topography, land-sea mask and runoff scheme manually every 500 years. In the PMIP4 last deglaciation Core experiment design, the bathymetry and land-sea mask are considered boundary conditions that cannot evolve automatically in the model. Thus, the decision of how often to make manual updates was left to the expert (Ivanovic et al., 2016). However, by varying the bathymetry in small steps, the artificial signals produced by changes in the ocean configuration might be reduced yielding to a more realistic representation of the ocean circulation and its interaction with the other climate components during the last deglaciation. It might be possible to produce a set of topographies in advance for several time slices with the aim of performing simulations with prescribed topography and ice sheets. However, when approaching the problem of simulations of the deglaciation with a fully interactive ice sheet-solid earth-climate model where the topographies and their changes are a prognostic variable, the need for an automatic procedure becomes more urgent. In such a model system, similar problems would also occur in long-term simulations of anthropogenic climate change. ~~.~~

Our long-term goal in the context~~In the frame~~ of the project "From the Last Interglacial to the Anthropocene: Modeling a Complete Glacial Cycle – (PalMod)", ~~our long-term goal~~ is to simulate the last termination with a coupled ice sheet-solid earth-climate model with interactive coastlines and topography forced only with solar insolation and greenhouse gases concentration. The planned model set up consists of the MPI-ESM (Giorgetta et al., 2013) coupled to the modified Parallel Ice Sheet Model (mPISM) and the Viscoelastic Lithosphere and Mantle model (VILMA). Hence, an automatic procedure to calculate a new set of masks, orographies and bathymetries together with adequate algorithms to transform the restart files that allows for the conservation of various properties is essential. The effect of orography changes on terrestrial runoff using a hydrological discharge (HD) model is treated as in Riddick et al. (2018). In this paper, we focus on interactive changes in ocean bottom topography and land-sea mask in the ocean component of MPI-ESM.

Dealing with interactive bathymetry and land-sea mask in ocean models is challenging from a technical point of view but is necessary for adequately simulating the last deglaciation with GCMs. Indeed, changes in bottom topography and oceanic boundaries during deglaciation were particularly large in the northern hemisphere (Fig. 1) where North Atlantic Deep Water formation takes place. Hence, they should be taken into consideration to get an appropriate representation of the deep ocean circulation during the last deglaciation. However, the generation of an ocean bathymetry to run a model usually implies several checks and manual corrections. This is a necessary step in order to, for example, avoid isolated wet points or inland lakes in the ocean domain. Additionally, it is crucial to look into details, whether passages, islands and peninsulas are correctly represented. If necessary, they should be modified by connecting artificial lakes ~~opening them~~ to the open ocean or connecting artificial islands ~~them~~ to the mainland. Repeating this manual procedure continuously is not feasible in very long-term simulations. Hence, to consider the effects of changing bottom topography and coastlines, it is essential to design an automatic procedure. Following this purpose, we present for the first time a tool allowing for the automatic computation of

bathymetry and land-sea mask changes in the Max Planck Institute Ocean Model (MPIOM). In our approach, we account for the conservation of mass and water properties at both, global and regional scales, thus avoiding artificial long-distance propagation of signals. The current version is tailored to a coarse resolution setup of MPIOM, but the extension to other setups is rather straightforward.

~~MPIOM is a free-surface ocean general circulation model with the hydrostatic and Boussinesq approximations. It solves the primitive equations on an Arakawa-C grid in the horizontal and a z-grid in the vertical (Maier-Reimer 1997). For freshwater, a mass-flux boundary condition is implemented. A detailed description of the model equations and its physical parametrizations is given in Marsland et al. (2003) while its performance as the ocean component of the MPI-ESM is evaluated by Jungclaus et al. (2013). MPIOM includes an embedded dynamic/thermodynamic sea-ice model (Notz et al., 2013) with a viscous-plastic rheology following Hibler (1979). In this paper, we use the MPIOM coarse grid configuration with a curvilinear orthogonal grid (GR30) and two poles (Haak et al., 2003), over Greenland and Antarctica. In the vertical, the model has 40 unevenly spaced levels, ranging from 15 meters near the surface to several hundred meters in the deep ocean.~~

The paper is organized as follows. The ocean model specifications to apply our algorithms is discussed in Sect. 2. The methodology for automatically changing the bathymetry and the land-sea mask in MPIOM is detailed in Sect. 3~~2~~. It contains the strategy to generate a coarse topography from a high-resolution data (Sect. 3~~2~~.1), the methodology to gradually change the bathymetry and land-sea mask along the last deglaciation (Sect. 3~~2~~.2), the solution for adjusting the ocean bottom floor in order to match changes in ocean volume and freshwater fluxes into the ocean (Sect. 3~~2~~.3), and the approach to modify the restart file with the aim of conserving mass and tracers when the ocean configuration changes (Sect. 3~~2~~.4). The behaviour of the algorithms within a transient simulation with MPI-ESM-1.2.00p4 is evaluated in Sect. 4~~3~~. Finally, the strengths and limitations of our approach and its applicability are discussed in Sect. 5.~~4.~~

2 Ocean model requirements

The algorithms presented in this paper are tailored for the coarse resolution setup of MPIOM but should be easily transferable to other model resolutions or other ocean models having similar assumptions and approximations. MPIOM is a free-surface ocean general circulation model with the hydrostatic and Boussinesq approximations and incompressibility is assumed. It solves the primitive equations on an Arakawa-C grid in the horizontal and a z-grid in the vertical (Maier-Reimer 1997). For freshwater, a mass-flux boundary condition is implemented. A detailed description of the model equations and its physical parametrizations is given in Marsland et al. (2003) while its performance as the ocean component of the MPI-ESM is evaluated by Jungclaus et al. (2013). MPIOM includes an embedded dynamic/thermodynamic sea-ice model (Notz et al., 2013) with a viscous-plastic rheology following Hibler (1979). Sea-ice is swimming in the water. Ice shelves are not included. In this paper, we use the MPIOM coarse resolution configuration with a curvilinear orthogonal grid (GR30) and

two poles (Haak et al., 2003), over Greenland and Antarctica. We decide to use the coarse configuration to reduce the computational time, but the algorithms presented in this paper can easily be adapted to higher resolution grids. In the vertical, the model has 40 unevenly spaced levels, ranging from 15 meters near the surface to several hundred meters in the deep ocean. Vertical discretization includes partial vertical grid cells. Therefore, at each horizontal grid point, the deepest wet cell has a thickness that is adjusted to resolve the discretized bathymetry. On the other hand, the surface layer thickness is also adjusted to account for the sea surface elevation and the sea ice/snow where appropriate.

~~3~~2 Methodology

As a starting point, we build the tool for automatically dealing with changes in bathymetry and land-sea mask for the coarse resolution configuration MPI-ESM-CR. This configuration is used for paleoclimate applications and corresponds to approximately 3 degrees horizontal resolution and 40 vertical levels (denoted as GR30) in the ocean component MPIOM. Despite the relatively coarse resolution, it is important to carefully consider the bathymetric details to avoid an unrealistic representation of the ocean floor. We pay particular attention to three aspects. First, we consider ~~look at~~ the land-sea mask with emphasis on the opening or closure of key straits and channels. Second, ~~we look at~~ the bathymetry of the same straits is treated in order to provide an adequate through-flow-depth (TFD). We assume here that to appropriately simulate~~resolve~~ the ocean circulation it is more important to conserve the correct~~obtain the right~~ TFD rather than the through-flow area. Having an adequate depth of the outflow (e.g. in the Strait of Gibraltar) ~~flow~~ yields a better representation of the water properties in our coarse resolution model. Finally, we check for the presence of lakes in the GR30 bathymetry; the Caspian Sea and the Black Sea (under LGM condition, for example) are the only cases that are permitted. Because we are dealing with an ocean model, we are interested in lakes that are connected to the ocean, that is the Black Sea. However, we include the Caspian Sea in our calculations because of its potential impact on the climate of Central Asia. Solving the SST of the Caspian Sea, which is much larger than other minor lakes, might be important for coupled climate simulations. All other lakes need to be removed from the ocean domain either by connecting them to the open ocean or by considering them as land. The atmospheric model component allows accounting for lakes on land (only the thermal component). In the framework of our model system, the adequate place to calculate water storage in lakes would be the hydrological discharge model, which is part of the land module.

Our aim is to perform the above-mentioned controls in an automatic way and, therefore, as a starting point, a high resolution (HR) bathymetry is necessary to obtain information on the small features. In what follows, we call HR a 10' × 10' gridded dataset. We use a remapped RTopo-2 bedrock topography for present-day conditions. RTopo-2 (Schaffer et al., 2016) is a compilation of consistent maps of global ocean bathymetry, upper and lower ice surface topographies and global surface height on a spherical grid with 0.5' horizontal resolution. The RTopo-2 topography was remapped to a 10' × 10' regular grid. Remapping the data, in this case, results from a compromise between the horizontal resolution and the computation time for

performing the algorithms, especially when reducing the resolution. Because the bathymetry and land-sea mask need to be adjusted several thousand times during deglaciation, it is crucial to construct a fast tool. The aim here is to speed up the computation by remapping RTopo-2 data without losing the general features. On the other hand, our next goal is to couple an ice-sheet and a solid earth model to MPI-ESM instead of prescribing the topography and ice thickness. The planned set up for the ice-sheet model consists of a horizontal regular resolution of 10 km and the output fields are then remapped to 10' × 10'. Therefore, we decide to work in this first approach with the same kind of input data. Still, to obtain a better description of the bathymetric details in regions which might be critical for the ocean circulation and water masses changes, the TFD values were modified in few straits. For this purpose, we use the TFD from SRTM30_PLUS (Becker at al., 2009) for the Strait of Gibraltar, Bab-el-Mandeb, Denmark Strait, Faroe-Shetland Channel, Northwest Passage and Nares Strait. The obtained values were used to modify the TFD of the corresponding regions of the remapped RTopo-2 topography. The resulting field is our reference topography for present-day conditions.

For the generation of the GR30 bathymetry during the last deglaciation, we use the ICE-6G_C reconstructions (Argus et al., 2014; Peltier et al., 2015). They contain information on topography, orography and masks derived from a global model of glacial isostatic adjustment constrained by data. In particular, the variable called "topography" consists of values of ocean bathymetry on ocean points and the land/ice-sheet surface on land points. The variable called "topography difference from present" is the anomaly of topography respect to present. Variables called "land area fraction" and "ice area fraction" represent the land-sea mask and ice-sea mask, respectively. Finally, the grounded ice-mask can be derived by multiplying the land area fraction and the ice area fraction. The horizontal resolution is 1° × 1° and the temporal resolution is 1 ka for the period spanning from 26 to 21 ka BP and 0.5 ka from 21 to 0 ka BP. Fields were interpolated to a 10' × 10' regular grid.

In order to preserve the small-scale structures from the HR topography for a particular time slice, we use the anomalies from ICE-6G_C relative to present and add them to our present HR topography. This is applied in ice-free areas only. As the surface of an ice sheet is rather smoothed, we use here directly the bilinearly interpolated ICE-6G_C topography data where ice is grounded. The two data sets are merged using the interpolated grounded ice mask as weights yielding our HR-topography for a particular time slice.

~~We believe that the correct solution is having a smoothed field in areas covered by ice (that are smoothed themselves) and a detailed field in areas free of ice. Therefore, the HR dataset for the last deglaciation was constructed by merging a) the interpolated ICE-6G_C fields of topography where ice is grounded (grounded ice-mask equal to 1) and b) the topography difference added to our reference topography for present day conditions elsewhere (grounded ice-mask equal to 0). We work with the reference data for present day in order to preserve the small topography features.~~

3~~2~~.1 Automatic generation of the GR30 bathymetry and land-sea mask

In this section, we describe the approach adopted to generate in an automatic way a bathymetry file to run MPIOM-GR30. Starting from a 10' × 10' gridded topography (HR) as the input file, our script executes the following steps:

(a) Generation of the HR land-sea mask. First, a raw version of the land-sea mask (*rawLSM*) is generated using the values of the input topography, assigning 1 to the ocean or wet grids (negative values of topography) and 0 to the land or dry grids (positive or zero values of topography). The resulting *rawLSM* is modified to prevent small inland lakes and isolated wet grid points. The strategy is to keep only the wet points that are directly connected to one of the following basins: World~~Atlantic-Pacific-Indian~~ Oceans, Mediterranean Sea, Red Sea, Black Sea and Caspian Sea. The wet points that are not connected to those basins are dried by assigning to them land-sea mask equal to 0. The result of this procedure is an HR land-sea mask in which only five basins are allowed to be wet and the smaller lakes are closed by assigning land to them.

(b) Generation of the GR30 land-sea mask. Reducing the resolution, in this case, can produce an unrealistic representation of the coastline due to the loss of details. Our strategy is to remap the HR land-sea mask to the GR30 MPIOM grid and then to modify it with focus on some specific features that are important for simulating the ocean circulation. We apply a first-order conservative remapping using the Climate Data Operator (CDO, 2015) to obtain values between 0 and 1 that we call "fraction ocean". The fraction ocean is, therefore, the fraction of the grid point that is wet. Then, we use that value to generate the GR30 land-sea mask taking into account the following aspects:

- A grid point is considered dry (land-sea mask equal to 0) if its value of fraction ocean is lower than 0.5.
- A grid point is considered wet (land-sea mask equal to 1) if its value of fraction ocean is larger or equal to 0.5 and if it is directly connected to one of the following basins: World~~Atlantic-Pacific-Indian~~ Oceans, Mediterranean Sea, Red Sea, Black Sea and Caspian Sea. We apply here a similar approach as for the HR land-sea mask. Starting from one point in each basin, the wet area is expanded if the adjacent grid points have fraction ocean larger or equal to 0.5. The algorithm is then repeated until there is no point left that meets the former conditions.
- There might still exist grid points with fraction ocean larger or equal to 0.5 which are not considered wet by the previous step because they are not directly connected to any of the five basins. Thus, they represent isolated wet areas in the coarse grid. Because isolated lakes were prevented in the HR land-sea mask, we assume that they are artificially enclosed by the remapping and therefore they are forced to be connected to the open ocean. The fraction ocean is used to decide about the path of the connection, and the land grids with the largest fraction ocean are flooded (land-sea mask to 1).
- Specific regions are considered~~examined~~ in detail for further checking and the GR30 land-sea mask is, therefore, ~~and~~ modified if necessary. First, we check if North and South America are connected by land or artificially separated by the remapping. Then, we check some straits or channels (Strait of Gibraltar, Bab-el-Mandeb, Bosphorus, Denmark

Strait, Faroe-Shetland Channel, Northwest Passage, Nares Strait and the Strait of Sicily), islands (Indonesia and Japan) and peninsulas (Florida, Thailand-Malaysia, Kamchatka, Italy and the Scandinavian Peninsula). The strategy here is to automatically control ~~look at the HR land-sea mask to evaluate~~ if the straits/channels are open or closed and if the islands/peninsulas are isolated from or connected to the mainland in the HR land-sea mask. To automatically perform this task, the algorithm finds the path of connection between two points apart. This is done in a restricted domain around the region of interest. For example, when checking the opening or closure of a strait, the points to be connected are wet points located in each side of the strait. If the algorithm finds that the path of connection between both points is always within the ocean, that means that the strait is open. Instead, if the path of connection is blocked by land, that means that the strait is closed. The location of each pair of points was manually and carefully decided for each region and is fixed in the code. It was tested that those points do not change from wet to dry or vice versa during the last deglaciation. The approach is applied to each specific region mentioned before and both resolutions, HR and GR30. ~~-~~ When necessary, the GR30 land-sea mask is regionally modified to be consistent with the HR data. The information of the fraction ocean is used to decide about the path of the opening or closure. Being the fraction ocean a float number it is highly unlikely to obtain multiple solutions. In that case, the algorithm would choose the first solution found.

(c) Generation of the GR30 bathymetry. As we are only interested in ocean depth and want to exclude potential effects of mountains on land, we multiply ~~First, only the values of ocean bottom topography from~~ the HR topography by the HR land-sea mask. This preserves the depth of ocean points and sets land values to 0 ~~field are kept by masking the land~~. Then, this HR ocean bathymetry is remapped to the GR30 MPIOM grid by applying a first-order conservative remapping. The resulting field is multiplied by the GR30 land-sea mask previously generated. Finally, the TFDs in some regions are modified according to the values of the HR bathymetry. The regions that are checked are the same as in the previous step. This way, the artificial smoothing created by the remapping is corrected in order to guarantee an adequate TFD. As it was mentioned before, we assume that it is more important to get a good representation of the TFD than of the area of the flow.

The resulting global GR30 bathymetry for present day is shown in Fig. 2b. Even though the resolution is coarse, the general features of both, the land-sea mask and depth compare well with the HR data (Fig. 2a). Two examples where the GR30 bathymetry is modified according to the values obtained for the HR one are plotted in Fig. 3. After remapping the land-sea mask, the Nares Strait resulted closed. This is an artificial effect because it appears open in the HR data (Fig. 3a). Therefore, the GR30 bathymetry was modified in order to open the Nares Strait (Fig. 3b) and the TFD there was set to 167 m according to the HR value. In the case of the Denmark Strait, the TFD in the GR30 resulted in 549 m after the remapping. It was set to 600 m (Fig. 3d) in correspondence of the HR value (Fig. 3c) in order to obtain an improved representation of regional features.

32.2 Time-dependent GR30 bathymetry and land-sea mask

One important aspect to consider when the bathymetry is being changed within a simulation, is to avoid sequences of rapid flooding and drying events of the shelves. We solve this issue by applying some resistance to change and thus, each new bathymetry field has a degree of dependency on the previous one. On the other hand, we limit the changes in both, ocean depth and land-sea mask in order to avoid abrupt transitions that can cause a model crash. As a result, changes in the ocean configuration are slow enough to allow the model to run without numerical instability. Here we made a compromise between the speed of changes and the reproduction of realistic features. Therefore, the approach described in Sect. 32.1 requires an adaptation to be applied subsequently in time. For each time slice in which the ocean configuration is being changed, the approach for the generation of the GR30 bathymetry is similar to the one previously described. The differences are the following:

- Two files (instead of one) are needed as input data for executing the script. They are the HR field of the current time slice and the GR30 field of the previous time slice.
- The fraction ocean derived from the remapping (*rawFraction*) is then modified to get the final fraction ocean (*Fraction*) by taking into consideration the previous GR30 land-sea mask (*preMask*) through an inertia coefficient (*Icoeff*) as follows:

$$Fraction = \begin{cases} Min(rawFraction + Icoeff\,; 1) & if\ preMask = 1 \\ Max(0\,; rawFraction - Icoeff) & if\ preMask = 0 \end{cases} \quad (1)$$

  where *Icoeff* is a dimensionless coefficient and can have values between 0 and 1. Based on sensitivity analysis, we decide to use an *Icoeff* equal to 0.1. In this way, the resulting fraction ocean keeps, to some degree, memory of the previous land-sea mask.
- Changes in the land-sea mask are limited. New wet (dry) points are open (closed) only if they are directly connected to land (ocean) in the previous topography. New potential islands start being dried with one grid point.
- Changes in depth are restricted to the value DH_{max} defined as:

$$DH_{max} = \begin{cases} dzw(1) & if\ it\ is\ a\ new\ wet\ point \\ dzw(1) - 3m & elsewhere \end{cases} \quad (2)$$

  where *dzw(1)* is the thickness of the first layer in MPIOM (15 m in our set up). The reason for this choice is that when accounting for the conservation of mass and tracers (Sect. 2.4.), large changes in depth can cause a negative thickness of the first layer of the model. This limitation does not affect the deep ocean where changes in bathymetry are slow but it can slow down the deepening or shallowing process of shelves.

To test the algorithms described in this section, the GR30 bathymetry from 21 ka BP to present day (forward in time) was generated. The HR dataset for the deglaciation previously described was interpolated in time to allow for the creation of a new GR30 bathymetry field every 10 years. The limitations in the changes of land-sea mask and depth are illustrated in Fig. 4 which shows time slices corresponding to the period when the Hudson Bay is being connected to the ocean. The black stars highlight the grid point where the process is initiated. The Hudson Bay is gradually opened and deepened by a slow process of flooding.

~~3~~2.3 Matching changes in ocean volume and freshwater fluxes into the ocean

The growth or decay of ice sheets and the resulting net freshwater flux into the ocean is the only responsible mechanism to change the volume of the ocean in MPIOM, as incompressibility is assumed. Otherwise, effects like thermal expansion could be important as well. When running the model with a fixed bathymetry, the net freshwater fluxes into the ocean affect the mean SSH and consequently the thickness of the uppermost ocean layer. When a new ocean bathymetry is derived in a formally independent process, the mass of water is distributed to the new configuration. Then, both estimates of the ocean volume should be consistent, and therefore, the mean SSH and mean thickness of the surface layer should be preserved within the simulation for all restart points. However, de facto, this is not always the case mainly for two reasons. On the one hand, the HR reconstructions might show inconsistencies if they do not exactly account for water conservation. On the other hand, reducing the resolution from HR to GR30 can cause disagreement in the ocean volume due to the loss of details in the bathymetry field. The aim of this step is to remove these two possible sources of inconsistencies. The procedure is to match the last GR30 ocean volume with the ocean volume of the new GR30 configuration, by performing the following steps:

~~Ocean bathymetry and land-sea mask change because the ice sheets grow or decay. Therefore, the net freshwater fluxes into the ocean should match the changes in ocean volume. This is not always the case mainly for two reasons. On the one hand, the HR reconstructions might show inconsistencies because they do not always account for water conservation. On the other hand, reducing the resolution from HR to GR30 can cause disagreements in the ocean volume due to the loss of details in the bathymetry field. It is important to note that changes in depth affect the thickness of the deepest layer in each grid point whereas the thickness of the uppermost ocean layer only depends on the sea surface height (SSH). This way, the mean SSH and, therefore, the mean thickness of the uppermost layer should be preserved along the simulation, which is important when considering conservation of heat capacity and exchanges with the atmosphere.~~

~~We adjust the ocean depth to keep the global mean SSH nearly constant along the simulation by performing the following steps:~~

The total volume of the ocean is computed before the generation of the new bathymetry (V_{old}). Both, the ocean depth and the modelled sea surface height (SSH) are considered for the calculation.

(a) The new ocean bathymetry and land-sea mask are generated as described in Sect. 3~~2~~.2. Then, the total ocean volume and area of the new configuration are computed (V_{new}; A_{new}).

(b) The new depth in each grid point is modified by adding the constant value C defined as:

$$C = \frac{(V_{old} - V_{new})}{A_{new}} \quad (3)$$

(c) The final changes in depth are again limited according to Eq. (2) to ensure model stability.

In this way, the resulting ocean GR30 bathymetry accounts for changes in the ocean volume due only to the freshwater fluxes into the ocean~~ocean volume is being adjusted every time that the bathymetry changes~~. There might exist slight discrepancies produced by the last step. However, by removing possible artificial changes in ocean volume, the~~distributing globally the volume change, this~~ procedure ensures that the mean SSH is reasonably well preserved, independently of the freshwater fluxes and the prescribed HR dataset.

3~~2~~.4 Adaptation of the restart file in order to conserve mass and tracers

The last modelled state of the ocean with its ocean configuration (restart file) will be used as the initial state for the later setup. Hence, the 2D and 3D fields should be adapted to the new bathymetry and land-sea mask. When carrying out this task, our aim is to account for the conservation of mass and tracers not only at global but also at regional scale. Therefore, the variables that are adapted in this step are SSH, sea-ice, snow on sea ice (for conserving mass) and tracers (for conserving them). From here on, when referring to tracers, we mean temperature, salinity and any passive tracer that MPIOM prognostically resolves (age tracer, radioactive tracer, CFC, etc.). The other model variables (like for example velocities) are not being modified. During the restart process, MPIOM multiplies the velocities with the land-sea mask, thus non-zero velocities are not a problem. However, on the coarse horizontal resolution applied in these very long climate model simulations, the velocities in the ocean are determined essentially by geostrophy and friction and after one month of simulation, the velocity field has adapted to the hydrographic fields. Our approach consists of the following steps:

(a) Vertical redistribution of water and tracers. In this first step, we keep the land-sea mask fixed and we only deal with changes in depth. 2D fields of SSH and 3D fields of tracers are vertically adjusted to the new depth. The strategy here is to conserve the volume and amount of tracers within the water column in each grid point. Considering an individual wet point, the SSH is modified according to the change in depth in order to preserve the ocean volume locally. For example, consider a wet grid point in which the depth is 120.44 meters and the SSH from the restart file is -0.71 meters. The height of the water column results in 120.44 – 0.71 meters and the vertical levels for this configuration are shown in Fig. 5a. After changing the bathymetry, the depth at the same grid point is 122.16 meters. Because the grid area is unchanged, the SSH is lowered to -2.43 meters to conserve the volume of the water column and the vertical levels are

adjusted as shown in Fig. 5b. As pointed out before, in MPIOM, the thickness of the uppermost or first layer depends on SSH, whereas the thickness of the deepest or last wet cell is adjusted to the bathymetry. The vertical distribution of all tracers is consistently moved along the vertical, taking into account the new layer thicknesses, in order to preserve the total amount of them within the water column. This involves the transfer of water and its properties between vertical adjacent boxes. The algorithm is formally identical to an advection using a first order upwind scheme with the depth changes being the product of time step and vertical velocity. The behaviour of the algorithms is displayed in Fig. 5 which shows an example of vertical profiles of temperature (Fig. 5c) and salinity (Fig. 5d). This way, the vertical profiles displayed in blue (Fig. 5c and d) are the ones from the original restart. The orange lines (Fig 5c and d) represent the original profiles shifted downward according to the change in depth. The resulting profiles after redistributing vertically the tracers to the new layer's thicknesses are displayed in green (Fig. 5d and d). Values of tracers are constant within each vertical layer of the model (stepped profile). As a result of deepening the bathymetry, the thickness of the bottom (surface) layer increase (decrease), whereas the middle layers remain unchanged (Figs. 5a and b). Therefore, to conserve tracers along the water column, vertical profiles are modified.

(b) ~~Vertical re-location of water and tracers. In this step, we keep the land-sea mask fixed and we only consider changes in depth. 2D fields of SSH and 3D fields of tracers are adjusted to the new depth. The strategy here is to conserve the volume and amount of tracers within the water column in each grid point. Looking at each wet point, the SSH is modified according to changes in depth. The distribution of tracers is consistently moved along the vertical, taking into account the new layers thickness.~~

(c) Horizontal smoothing. The previous step is applied to each wet grid point independently, considering only changes in depth. Therefore, the resulting SSH field might present ~~Large SSH depressions can result from the previous step producing a negative thickness of the first layer in MPIOM. To avoid~~ large gradients between adjacent grid points, which could lead to numerical instability when inserted into MPIOM. To fix this, the SSH field is smoothed by taking into consideration the conservation of mass and tracers. That is, when necessary, values of SSH are modified by moving a volume of water with its tracer properties ~~a certain amount of tracers~~ between adjacent ocean grid points. The maximum permitted horizontal SSH gradient between neighbouring points is set to 0.2 meters, which seems to ensure numerical stability in the ocean model.

(d) Horizontal re-location of water, tracers, sea ice and snow on sea ice when the land-sea mask changes. In step (a) we describe the procedure for dealing with changes in depth only. In this step, the new wet (dry) points resulting from changes in the land-sea mask are filled (emptied). We avoid performing any kind of interpolation in this stage because it would not account for conservation of mass and tracers. Instead, in ~~In~~ order to conserve properties, the necessary amount of water and tracers to fill new wet points is taken from other boxes. The simplest approach would be to take water from all ocean boxes. However, this would involve the artificial long-distance transfer of water mass properties.

Therefore, we decide to use only adjacent ocean boxes. That is, small volumes of water with its properties coming from adjacent points is placed into the new wet point until completely filling it. Similarly, the amount of water and tracers from a point which is dried is re-located among the neighbouring wet grid points. This operation is repeated for sea ice and snow on sea ice. There needs to be a compromise between involving only a few neighbouring grid points and the risk of obtaining large horizontal gradients of SSH. Sensitivity tests were performed to achieve the optimal balance for both, filling and emptying procedures.

(e) Horizontal smoothing. Again, we apply step (b) to obtain a sufficiently smooth SSH field to ensure numerical stability when running the model.

An example of the above-described approach is illustrated in Fig. 6~~5~~, which shows regional SSH fields during an arbitrary time slice of the last deglaciation, when the north of Europe is still partially covered by ice. The SSH field from the original restart file is plotted in Fig. 6a~~5a~~. Then, the ocean bottom was deepened along the shelf due to a decay of the ice sheets. Accordingly, the SSH values after the vertical redistribution~~re-location~~ (Fig. 6b~~5b~~) are lower than the original ones (Fig. 6a~~5a~~). The land-sea mask also changed, there are a new wet and dry grid points (coloured in yellow and pink, respectively, in Fig. 6c~~5c~~). When drying a point, the amount of water is horizontally re-located among its neighbours resulting in a raised SSH in the surrounding area (red in Fig. 6c~~5c~~). Conversely, a lowered (blue in Fig. 6c~~5c~~) SSH field results when a grid point is flooded. A smoothing of the SSH field constitutes the last step to obtain the final field (Fig. 6d~~5d~~).

This approach guarantees the conservation of mass and tracers in the open ocean. The algorithms are not being applied in lakes (Caspian Sea and Black Sea when it is not connected to the open ocean) and therefore they constitute an exception for the conservation of water properties. MPIOM does not account for freshwater fluxes in lakes in order to avoid eventual over-flooding or drying them out. However, our algorithms could still be improved to take this aspect into consideration.

~~4~~3 Transient simulation

This section has the aim of testing the above-described tool in a long-term run with MPI-ESM. The purpose is not to analyse the climate response to a changing bathymetry and land-sea mask, this will be discussed in a consecutive paper. The aim of this experiment is evaluating the performance of the tool in terms of model stability and conservation of mass and tracers. This is a necessary step towards a fully coupled simulation with interactive ice sheets.

We performed a simulation with MPI-ESM from 21 ka BP to 7 ka BP. The ICE6-G_C reconstructions were used to derive the HR topography as detailed in the beginning of Sect. 3~~2~~. They were linearly interpolated in time to obtain changes in the bathymetry and land-sea mask every 10 years. In this way, the tool was applied 1400 times within the run and was tested under a wide range of conditions. The interpolated ICE6-G_C reconstructions were also used to compute the time-dependent freshwater fluxes into the ocean. First, the 10-year interval ~~instantaneous~~ time derivative of the gridded ice thickness is

calculated. Only the ice-sheet thicknesses at grounded points are ~~thickness of the grounded-ice sheets is~~ considered. The time rate of change of this quantity ~~resulting value~~ is then divided by the density ratio between ice and freshwater~~water~~ to obtain the extra freshwater flux into the ocean:

$$F_{freshwater}(x,y,t) = \frac{-1}{R}\frac{\partial Ice(x,y,t)}{\partial t} \qquad (4)$$

where *Ice* is the ice thickness of the grounded-ice sheets and *R* the density ratio between ice and freshwater~~water~~. The resulting value is considered constant for a period of 10 years, although it is introduced to the model every time step. The extra freshwater is ~~freshwater fluxes are~~ transported into the ocean through the hydrological discharge (HD) model which considers the changes in river routing (Riddick et al., 2018). Hence, while the ice sheets melt, the ocean receives a positive net freshwater flux and the bottom topography and land-sea mask adapt to it. As a consequence, both the ocean volume and the ocean surface area increase in time. The relative changes of ocean volume and area along the simulation are plotted in Fig. 7~~6~~. The ocean volume in the beginning and at the end of the run is equal to 1.2858×10^{18} m^3 and 1.3313×10^{18} m^3, respectively. These values represent a relative increase of approximately 3.58 % (Fig. 7a~~6a~~). The ocean surface area changed from 3.3692×10^{14} m^2 to 3.6089×10^{14} m^2 in the period of the simulation. This accounts for a relative change of 7.11 % (Fig. 7b~~6b~~) produced by changes in the land-sea mask. The rate of change increases from 14.5 ka BP onward, in response to the massive ice-sheet decay. There is a slight relative decrease in the ocean surface area by the end of the simulation, around 7200 yrs BP (Fig. 7b~~6b~~). This is because few grid points in the north of Canada were dried in that period due to uplift as consequence of glacial isostatic adjustment. Therefore, even though flooding events are dominant during the deglaciation, this particular case constitutes a test for drying points as well.

To illustrate the evolution of a prognostic variable computed within the ocean component of the MPI-ESM, Fig. 8~~7~~ shows the sea surface temperature (SST, ºC) at different time slices. Changes in the land-sea mask can also be observed. For instance, the LGM (Fig. 8a~~7a~~) is characterized by the large extent of ice sheets considered as land by the model. The Black Sea is isolated and therefore, it is solved as a lake. Around 13 ka BP (Fig. 8b~~7b~~), the Scandinavian and the Siberian ice sheets are almost melted and the Antarctic ice sheet begins to retreat. The Laurentide ice sheet starts to melt and the Black Sea gets connected to the Mediterranean Sea around 10 ka BP (Fig. 8c~~7c~~). Conditions close to present-day are reached by the end of the simulation (Fig. 8d~~7d~~) when the Hudson Bay is open. The model is able to deal with a changing ocean configuration and computes the SST fields while the bathymetry and land-sea mask change.

The changes of ocean volume should match the freshwater fluxes into the ocean in order to account for water conservation. On the one hand, the differences in ocean volume derived from two consecutive restart files (10 years difference) were computed. We do not account for lakes in this calculation. The resulting time series is plotted in Fig. 9a~~8a~~ (black line). On the other hand, for the same period of time, the freshwater fluxes into the ocean were integrated. This is, the monthly fields of freshwater input were multiplied by the grid area and by the number of seconds in that month. The resulting values were horizontally and temporally (each 10 years) integrated to obtain the total freshwater fluxes into the ocean in m^3 (Fig. 9a~~8a~~,

red line). Both curves are almost identical indicating that changes in ocean volume are indeed only caused by the freshwater input. The difference between both time series was divided by the ocean area in order to obtain the errors in the mean sea level (Fig. 9b~~8b~~). They are of the order of 1×10^{-3} cm and within the computational accuracy. Therefore, the changes in ocean volume match the freshwater input indicating that water is being conserved. Note that MPIOM uses the incompressibility assumption and therefore, the contribution of the thermal expansion on SSH is not being considered here. The year when the Black Sea is connected to the Mediterranean Sea, around 10.3 ka BP, is an exception for the conservation. This is because in our approach we do not account for the conservation of water and tracers inside lakes. Therefore, when computing changes in the ocean volume, the water from the Black Sea is being introduced in the computation producing a large peak (Fig. 9a~~8a~~) that does not match with the freshwater input of that year.

Another aspect to check in the simulation is the conservation of water properties. Even if the ocean volume changes due to the freshwater input (Fig. 7~~6~~), the global inventory of tracers should be constant in the absence of sources or sinks. The yearly mean of the global salt content was calculated for the period of the simulation using the model output written in 32 bits. Lakes are not being considered in the calculation. Figure 10~~9~~ shows the relative change between two consecutive years. Relative errors are less than 1×10^{-7} and can be considered within the computational error as it is the same accuracy for the model outputs. Because we use an identical approach for all the tracers (including salinity), we are confident that the global content of tracers is conserved in the long-term simulation with MPI-ESM. Again, the year when the Black Sea is connected to the Mediterranean Sea is an exception for the conservation of tracers.

As described in Sect. 3~~2~~.3, the ocean bottom depth is adjusted in order to match changes in the ocean volume and the freshwater fluxes into the ocean. During this process, the mean SSH should remain unchanged. To evaluate the performance of the algorithms in dealing with this, the mean SSH was computed each time the restart files were modified. The calculation is done, therefore, every 10 years and the results are plotted in Fig. 11a~~10a~~. Deviations from a constant value are lower than 4 cm indicating that our approach is effective in maintaining the mean SSH unchanged. Figure 11b~~10b~~ shows the mean SSH computed from the 10-years mean fields. The model runs for 10 years with the same ocean bathymetry and land-sea mask. Therefore, during that period, the ocean depth is not being adjusted to the unbalanced freshwater input. This causes changes in the mean SSH. Still, differences are low and the maximum deviation from zero is 30 cm (around 14.5 ka BP, Fig. 11b~~10b~~) in response to a very large freshwater flux. Considering that changing the bathymetry according to the freshwater fluxes corrects these inconsistencies (Fig. 11a~~10a~~), the tool could be applied more often within the simulation in order to improve the results. Nevertheless, we consider that these deviations are small and that a time step of 10 years is an optimal compromise between computing time and model performance.

5~~4~~ Remarks

In this paper, we presented the strategy which we followed to automatically change the ocean bathymetry and land-sea mask in MPIOM, the ocean component of the MPI-ESM. The procedure for both, the generation of the bathymetry file and the adaptation of the restart file were described in details. The simulation presented here had the aim of evaluating the performance of the tool in terms of model stability and conservation of water properties. The algorithms showed very good behaviour for a long-term simulation and our approach guarantees the conservation of mass and tracers.

The principal tool consists of shell scripts that are called with a maximum of three input files. All the calculations are performed with CDO commands and programs written in FORTRAN. The tool can easily be included at the end of the main run script without the necessity of interrupting the simulation. There are two shell scripts that need to be called after the restart file is written by the model. The first one generates the new bathymetry file for running MPIOM. Two input files are required to run this script. The first one corresponds to a NetCDF file containing the new HR bathymetry. The second input is an ASCII file which corresponds to the previous GR30 bathymetry as it was read by MPIOM. The output of this shell script is an ASCII file containing the new GR30 bathymetry to be read by the model. As a result, this script replaces the old bathymetry file to run MPIOM with the new one. The second shell script adapts the restart file generated by the model to the new ocean configuration. This script needs three input files. The first and second ones correspond to the old and new bathymetry files as read by MPIOM, respectively. The last input is the restart file generated by the model in NetCDF format. The output is the modified restart file in NetCDF format to replace the original one. The execution of this tool needs the restart file generated by the model as input. Therefore, it can be called only after a restart file is generated. Contrary, it is possible to resubmit the job without applying the tool, that is with fixed bathymetry, land-sea mask and, therefore, unmodified restart file. This allows for a shorter number of years between resubmissions than the ones required for changing the bathymetry. Consequently, the tool is easy to apply and it is fast, taking less than a minute to run on a workstation.

~~The principal tool consists of shell scripts that are called with a maximum of three input files. All the calculations are performed with CDO commands and programs written in FORTRAN. Consequently, the tool is easy to apply and it is fast, taking less than a minute to run on a workstation.~~

There are mainly three limitations in our technique. First, the fact that changes in depth and coastlines are limited can slow down the flooding and drying events of the shelves. However, it is important to note that changes in topography in response to the ~~Thus, the duration of strong events of~~ ice-sheet retreat and isostatic adjustments are solved neither by the ocean model MPIOM nor by our algorithms. Instead, the HR topography is prescribed to our tool or solved by the ice-sheet model. In this sense, the non-linear changes or abrupt events that occurred during the last deglaciation are not affected by our methodology. Still, if the timing of the flooding and drying events of the shelves ~~might be affected. If this~~ is considered to be critical, the algorithms could be applied more often within the simulation (every year, for example). However, in MPI-ESM, changing the topography implies also changes in the river routing and the land mask for the atmospheric model. Therefore, there should be a compromise between the frequency that topography is being changed and the computational time. From our results, we conclude that changing the bathymetry every 10 years during the last deglaciation in our coarse resolution model

is an optimal compromise between both, model performance and computing time. Another possibility would be to widen the stencil used for collecting water for new ocean points. This would allow a faster propagation of coastlines by more than one grid point per iteration. This might also turn out to be necessary when applying the tool to ocean configurations with higher horizontal resolution. Second, this tool was originally written for the curvilinear orthogonal grid (GR) with two poles. Although we presented in this paper the results for the coarse resolution GR30, the tool can be also applied for the low resolution (GR15) configuration of MPIOM. Still, for the moment its usage is limited to GR grids. We are currently working on a new version to include the tripolar (TP) quasi-isotropic grid (Murray, 1996) among the applications. In general, the algorithms are easily adapted to any ocean model that meets the same requirements as MPIOM: Arakawa-C grid in the horizontal, z-grid in the vertical including partial bottom cells, free-surface and mass flux boundary conditions. However, there are some parameters inside the scripts that depend on the grid. They are the location of each pair of points in order to perform the checking steps described in Sect. 3.1 for correcting the bathymetric details. Third, our approach cannot guarantee the conservation of mass and tracers inside lakes. This is our first version and algorithms will be improved to include the lakes in the calculations, in particular, when the restart file is modified in order to fully conserve mass and tracers.

Despite the limitations mentioned above, this is, to our knowledge, the first time that changes in ocean bottom topography and coastlines are interactively computed in an ocean model for simulating the last deglaciation. Therefore, the presented modules constitute a step forward towards a realistic long-term simulation covering periods with strong topographic changes~~simulation~~. We are currently continuing our efforts in the direction of an interactive coupling between MPI-ESM and the ice-sheet model. Our goal is to combine single components into a fully coupled ice sheet-solid earth-climate model with interactive coastlines and topography forced only with solar insolation and greenhouse gas concentrations.

65 Code and data availability

A version of the code is available under the 3-Clause BSD License on Zenodo at https://doi.org/10.5281/zenodo.1249579. The MPI-ESM is available under the Software License Agreement version 2, after acceptance of a licence (https://www.mpimet.mpg.de/en/science/models/license/). The ICE-6G_C reconstructions used in this paper are freely accessible through the website: http://www.atmosp.physics.utoronto.ca/~peltier/data.php.

Author contributions. UM had the original idea, performed the experiment and coordinated the work. VLM developed the algorithms, made the analysis and figures and prepared the manuscript with contribution from UM.

Competing interests. The authors declare that they have no conflict of interest.

Acknowledgements. This work was funded by the German Federal Ministry of Education and Research (BMBF) through PalMod project, grant No. 01LP1513C. Special thanks to Anne Mouchet and Helmuth Haak for their comments and suggestions that helped to improve the manuscript.

References

Abe-Ouchi, A., Saito, F., Kawamura, K., Raymo, M. E., Okuno, J. I., Takahashi, K., and Blatter, H.: Insolation-driven 100,000-year glacial cycles and hysteresis of ice-sheet volume, Nature, 500, 190-194, 2013.

Abe-Ouchi, A., Saito, F., Kageyama, M., Braconnot, P., Harrison, S. P., Lambeck, K., Otto-Bliesner, B. L., Peltier, W. R., Tarasov, L., Peterschmitt, J.-Y., and Takahashi, K.: Ice-sheet configuration in the CMIP5/PMIP3 Last Glacial Maximum experiments, Geosci. Model Dev., 8, 3621-3637, https://doi.org/10.5194/gmd-8-3621-2015, 2015.

Annan, J. D. and Hargreaves, J. C.: A new global reconstruction of temperature changes at the Last Glacial Maximum, Clim. Past, 9, 367-376, doi:10.5194/cp-9-367-2013, 2013.

Argus, D. F., Peltier, W. R., Drummond, R., and Moore, A. W.: The Antarctica component of postglacial rebound model ICE-6G_C (VM5a) based on GPS positioning, exposure age dating of ice thicknesses, and relative sea level histories, Geophys. J. Int., 198, 537-563, doi:10.1093/gji/ggu140, 2014.

Becker, J. J., Sandwell, D. T., Smith, W. H. F., Braud, J., Binder, B., Depner, J., Fabre, D., Factor, J., Ingalls, S,. Kim, S-H., Ladner, R., Marks, K., Nelson, S., Pharaoh, A., Trimmer, R., Von Rosenberg, J., Wallace, G., and Weatherall. P.: Global Bathymetry and Elevation Data at 30 Arc Seconds Resolution: SRTM30_PLUS, Mar. Geod., 32:4, 355-371, 2009.

Bereiter, B., Eggleston, S., Schmitt, J., Nehrbass-Ahles, C., Stocker, T. F., Fischer, H., Kipfstuhl, S., and Chappellaz, J.: Revision of the EPICA Dome C CO 2 record from 800 to 600 kyr before present, Geophys. Res. Lett., 42, 542-549, doi:10.1002/2014GL061957, 2015.

Berger, A.: Long-Term Variations of Daily Insolation and Quaternary Climatic Changes, J. Atmos. Sci., 35, 2362–2367, doi:10.1175/1520-0469(1978)035<2362:LTVODI>2.0.CO;2, 1978.

Bonelli, S., Charbit, S., Kageyama, M., Woillez, M.-N., Ramstein, G., Dumas, C., and Quiquet, A.: Investigating the evolution of major Northern Hemisphere ice sheets during the last glacial-interglacial cycle, Clim. Past, 5, 329-345, doi:10.5194/cp-5-329-2009, 2009.

Boulton, G. S., Dongelmans, P., Punkari, M., and Broadgate, M.: Palaeoglaciology of an ice sheet through a glacial cycle: the European ice sheet through the Weichselian, Quaternary Sci. Rev., 20, 591–625, doi:10.1016/S0277-3791(00)00160-8, 2001.

Braconnot, P., Otto-Bliesner, B., Harrison, S., Joussaume, S., Peterchmitt, J.-Y., Abe-Ouchi, A., Crucifix, M., Driesschaert, E., Fichefet, Th., Hewitt, C. D., Kageyama, M., Kitoh, A., Laîné, A., Loutre, M.-F., Marti, O., Merkel, U., Ramstein, G., Valdes, P., Weber, S. L., Yu, Y., and Zhao, Y.: Results of PMIP2 coupled simulations of the Mid-Holocene and Last Glacial Maximum – Part 1: experiments and large-scale features, Clim. Past, 3, 261-277, https://doi.org/10.5194/cp/3-261-2007, 2007a.

Braconnot, P., Otto-Bliesner, B., Harrison, S., Joussaume, S., Peterchmitt, J.-Y., Abe-Ouchi, A., Crucifix, M., Driesschaert, E.,Fichefet, Th., Hewitt, C. D., Kageyama, M., Kitoh, A., Loutre, M.-F., Marti, O., Merkel, U., Ramstein, G., Valdes, P., Weber, L., Yu, Y., and Zhao, Y.: Results of PMIP2 coupled simulations of the Mid-Holocene and Last Glacial Maximum – Part 2: feedbacks with emphasis on the location of the ITCZ and mid and high latitudes heat budget, Clim. Past, 3, 279-296, https://doi.org/10.5194/cp-3-279-2007, 2007b.

Brady, E. C., Otto-Bliesner, B. L., Kay, J. E., and Rosenbloom, N.: Sensitivity to Glacial Forcing in the CCSM4, J. Climate, 26, 1901-1925, 2013.

Briggs, R. D., Pollard, D., and Tarasov, L.: A data-constrained large ensemble analysis of Antarctic evolution since the Eemian, Quaternary Sci. Rev., 103, 91-115, doi:10.1016/j.quascirev.2014.09.003, 2014.

Buizert, C., Gkinis, V., Severinghaus, J. P., He, F., Lecavalier, B. S., Kindler, P., Leuenberger, M., Carlson, A. E., Vinther, B., Masson-Delmotte, V., White, J. W. C., Liu, Z., Otto-Bliesner, B., and Brook, E. J.: Greenland temperature response to climate forcing during the last deglaciation, Science, 345, 1177-1180, doi:10.1126/science.1254961, 2014.

CDO: Climate Data Operators. Available at: http://www.mpimet.mpg.de/cdo, 2015.

Dyke, A. S., Andrews, J. T., Clark, P. U., England, J. H., Miller, G. H., Shaw, J., and Veillette, J. J.: The Laurentide and Innuitian ice sheets during the Last Glacial Maximum, Quaternary Sci. Rev., 21, 9-31, doi:10.1016/S0277-3791(01)00095-6, 2002.

Ganopolski, A., Winkelmann, R., Schellnhuber, H. J.: Critical insolation–CO2 relation for diagnosing past and future glacial inception. Nature, 529 (7585): 200 DOI:10.1038/nature16494, 2016.

Giorgetta, M. A., Johann Jungclaus, J., Reick, C. H., Legutke, S., Bader, J., Böttinger, M., Brovkin, V., Crueger, T., Esch., M., Fieg, K., Glushak, K., Gayler, V., Haak, H., Hollweg, H.-D., Ilyina, T., Kinne, S., Kornblueh, L., Matei, D., Mauritsen, T., Mikolajewicz, U., Mueller, W., Notz, D., Pithan, F., Raddatz, T., Rast, S., Redler, R., Roeckner, E., Schmidt, H., Schnur, R., Segschneider, J., Six, K. D., Stockhause, M., Timmreck, C., Wegner, J., Widmann, H., Wieners, K.-H., Claussen, M., Marotzke, J., and Stevens, B.: Climate and carbon cycle changes from 1850 to 2100 in MPI-ESM

simulations for the Coupled Model Intercomparison Project phase 5, J. Adv. Model. Earth Syst., 5, 572597, doi:10.1002/jame.20038, 2013.

Haak, H., Jungclaus, J., Mikolajewicz, U., and Latif, M.: Formation and propagation of great salinity anomalies. Geophys. Res. Lett., 30(9): 1473, pp. 26-1-26-4. doi:10.1029/2003GL017065, 2003.

Heinemann, M., Timmermann, A., Elison Timm, O., Saito, F., and Abe-Ouchi, A.: Deglacial ice sheet meltdown: orbital pacemaking and CO2 effects, Clim. Past, 10, 1567-1579, doi:10.5194/cp-10-1567-2014, 2014.

Hibler, W. D.: A dynamic thermodynamic sea ice model, J. Phys. Oceanogr., 9(4), 815-846, 1979.

Ivanovic, R. F., Gregoire, L. J., Kageyama, M., Roche, D. M., Valdes, P. J., Burke, A., Drummond, R., Peltier, W. R., and Tarasov, L.: Transient climate simulations of the deglaciation 21–9 thousand years before present (version 1) – PMIP4 Core experiment design and boundary conditions, Geosci. Model Dev., 9, 2563-2587, https://doi.org/10.5194/gmd-9-2563-2016, 2016.

Jouzel, J., Masson-Delmotte, V., Cattani, O., Dreyfus, G., Falourd, S., Hoffmann, G., Minster, B., Nouet, J., Barnola, J. M., Chappellaz, J., Fischer, H., Gallet, J. C., Johnsen, S., Leuenberger, M., Loulergue, L., Luethi, D., Oerter, H., Parrenin, F., Raisbeck, G., Raynaud, D., Schilt, A., Schwander, J., Selmo, E., Souchez, R., Spahni, R., Stauffer, B., Steffensen, J. P., Stenni, B., Stocker, T. F., Tison, J. L., Werner, M., and Wolff, E. W.: Orbital and Millennial Antarctic Climate Variability over the Past 800000 Years, Science, 317, 793-796, doi:10.1126/science.1141038, 2007.

Jungclaus, J. H., Fischer, N., Haak, H., Lohmann, K., Marotzke, J., Matei, D., Mikolajewicz, U., Notz, D., and vonStorch, J. S.: Characteristics of the ocean simulations in MPIOM, the ocean component of the MPI-Earth system model, J. Adv. Model Earth Syst., 5, 422-446, doi:10.1002/jame.20023, 2013.

Justino, F., Timmermann, A., Merkel, U., and Souza, E. P.: Synoptic Reorganization of Atmospheric flow during the Last Glacial Maximum, J. Climate, 18, 2826-2846, 2005.

Kageyama, M., Braconnot, P., Harrison, S. P., Haywood, A. M., Jungclaus, J., Otto-Bliesner, B. L., Peterschmitt, J.-Y., Abe-Ouchi, A., Albani, S., Bartlein, P. J., Brierley, C., Crucifix, M., Dolan, A., Fernandez-Donado, L., Fischer, H., Hopcroft, P. O., Ivanovic, R. F., Lambert, F., Lunt, D. J., Mahowald, N. M., Peltier, W. R., Phipps, S. J., Roche, D. M., Schmidt, G. A., Tarasov, L., Valdes, P. J., Zhang, Q., and Zhou, T.: The PMIP4 contribution to CMIP6 – Part 1: Overview and over-arching analysis plan, Geosci. Model Dev., 11, 1033-1057, https://doi.org/10.5194/gmd-11-1033-2018, 2018.

Kim, S.-J.: The effect of atmospheric CO 2 and ice sheet topography on LGM climate, Clim. Dynam., 22, 639-651, 2004.

Klockmann, M., Mikolajewicz, U., and Marotzke, J.: The effect of greenhouse gas concentrations and ice sheets on the glacial AMOC in a coupled climate model, Climate of the Past, 12, 1829-1846, 2016.

Lambeck, K., Rouby, H., Purcell, A., Sun, Y., and Sambridge, M.: Sea level and global ice volumes from the Last Glacial Maximum to the Holocene, P. Natl. Acad. Sci., 111, 15296-15303, doi:10.1073/pnas.141176211, 2014.

Liu, Z., Otto-Bliesner, B. L., He, F., Brady, E. C., Tomas, R., Clark, P. U., Carlson, A.. E., Lynch-Stieglitz, J., Curry, W., Brook, E., Erickson, D., Jacob, R., Kutzbach, J., and Cheng, J.: Transient Simulation of Last Deglaciation with a New Mechanism for Bølling-Allerød Warming, Science, 325, 310-314, doi:10.1126/science.1171041, 2009.

Loulergue, L., Schilt, A., Spahni, R., Masson-Delmotte, V., Blunier, T., Lemieux, B., Barnola, J.-M., Raynaud, D., Stocker, T. F., and Chappellaz, J.: Orbital and millennial-scale features of atmospheric CH 4 over the past 800000 years, Nature, 453, 383-386, doi:10.1038/nature06950, 2008.

Maier-Reimer, E.: Design of a closed boundary regional model of the Arctic Ocean. Bull. Amer. Meteor. Soc. Workshop on polar processes in global climate, 13-15 Nov, 1996, 72-73, 1997.

Marcott, S. A., Bauska, T. K., Buizert, C., Steig, E. J., Rosen, J. L., Cuffey, K. M., Fudge, T. J., Severinghaus, J. P., Ahn, J., Kalk, M. L., McConnell, J. R., Sowers, T., Taylor, K. C., White, J. W. C., and Brook, E. J.: Centennial-scale changes in the global carbon cycle during the last deglaciation, Nature, 514, 616-619, doi:10.1038/nature13799, 2014.

Marsland, S. J., Haak, H., Jungclaus, J. H., Latif, M., and Roske, F.: The Max Planck Institute global ocean/sea ice model with orthogonal curvilinear coordinates, Ocean Model., 5, 91–127, 2003.

Menviel, L., Timmermann, A., Timm, O. E., and Mouchet, A.: Deconstructing the Last Glacial termination: the role of millennial and orbital-scale forcings, Quaternary Sci. Rev., 30, 1155-1172, doi:10.1016/j.quascirev.2011.02.005, 2011.

Mikolajewicz, U., Gröger, M., Maier-Reimer, E., Schurgers, G., Vizcaíno, M., and Winguth, A.: Long-term effects of anthropogenic CO2 emissions simulated with a complex earth system model, Clim. Dynam., 28, 599-633, doi:10.1007/s00382-006-0204-y, 2007a.

Mikolajewicz, U., Vizcaíno, M., Jungclaus, J., and Schurgers, G.: Effect of ice sheet interactions in anthropogenic climate change simulations, Geophys. Res. Lett., 34, doi:10.1029/2007GL031173, 2007b.

Murray, R. J.: Explicit generation of orthogonal grids for ocean models. J. Comput. Phys., 126, 251-273, 1996.

Notz, D., Haumann, F. A., Haak, H., Jungclaus, J. H., and Marotzke, J.: Arctic sea-ice evolution as modeled by Max Planck Institute for meteorology's Earth system model, J. Adv. Model. Earth Syst., 5, 173-194, doi:10.1002/jame.20016, 2013.

Otto-Bliesner, B. L., Russell, J. M., Clark, P. U., Liu, Z., Overpeck, J. T., Konecky, B., deMenocal, P., Nicholson, S. E., He, F., and Lu, Z.: Coherent changes of southeastern equatorial and northern African rainfall during the last deglaciation, Science, 346, 1223-1227, doi:10.1126/science.1259531, 2014.

Pausata, F. S. R., Li, C., Wettstein, J. J., Kageyama, M., and Nisancioglu, K. H.: The key role of topography in altering North Atlantic atmospheric circulation during the last glacial period, Clim. Past, 7, 1089-1101, doi:10.5194/cp-7-1089-2011, 2011.

Peltier, W. R., Argus, D. F., and Drummond, R.: Space geodesy constrains ice age terminal deglaciation: The global ICE-6G_C (VM5a) model, J. Geophys. Res.-Sol. Ea., 120, 450-487, doi:10.1002/2014JB011176, 2015.

Riddick, T., Brovkin, V., Hagemann, S., and Mikolajewicz, U.: Dynamic hydrological discharge modelling for coupled climate model simulations of the last glacial cycle, Geosci. Model Dev. Discuss., https://doi.org/10.5194/gmd-2018-10, in review, 2018.

Ridley, J. K., Huybrechts, P., Gregory, J. M., and Lowe, J. A.: Elimination of the Greenland Ice Sheet in a High CO2 Climate, J. Climate, 18, 3409-3427, doi:10.1175/JCLI3482.1, 2005.

Roche, D. M., Renssen, H., Paillard, D., and Levavasseur, G: Deciphering the spatio-temporal complexity of climate change of the last deglaciation: a model analysis, Clim. Past, 7, 591-602, doi:10.5194/cp-7-591-2011, 2011.

Schaffer, J., Timmermann, R., Arndt, J. E., Kristensen, S. S., Mayer, C., Morlighem, M., and Steinhage, D.: A global, high-resolution data set of ice sheet topography, cavity geometry, and ocean bathymetry, Earth Syst. Sci. Data, 8, 543-557, https://doi.org/10.5194/essd-8-543-2016, 2016.

Svendsen, J. I., Alexanderson, H., Astakhov, V. I., Demidov, I., Dowdeswell, J. A., Funder, S., Gataullin, V., Henriksen, M., Hjort, C., Houmark-Nielsen, M., Hubberten, H. W., Ingólfsson, Ó., Jakobsson, M., Kjær, K. H., Larsen, E., Lokrantz, H., Lunkka, J. P., Lyså, A., Mangerud, J., Matiouchkov, A., Murray, A., Möller, P., Niessen, F., Nikolskaya, O., Polyak, L., Saarnisto, M., Siegert, C., Siegert, M. J., Spielhagen, R. F., and Stein, R.: Late Quaternary ice sheet history of northern Eurasia, Quaternary Sci. Rev., 23, 1229-1271, doi:10.1016/j.quascirev.2003.12.008, 2004.

Tarasov, L., Dyke, A. S., Neal, R. M., and Peltier, W. R.: A data-calibrated distribution of deglacial chronologies for the North American ice complex from glaciological modeling, Earth Planet. Sci. Lett., 315–316, 30-40, doi:10.1016/j.epsl.2011.09.010, 2012.

Ziemen, F. A., Rodehacke, C. B., and Mikolajewicz, U.: Coupled ice sheet-climate modeling under glacial and pre-industrial boundary conditions, Clim. Past, 10, 1817-1836, doi:10.5194/cp-10-1817-2014, 2014.

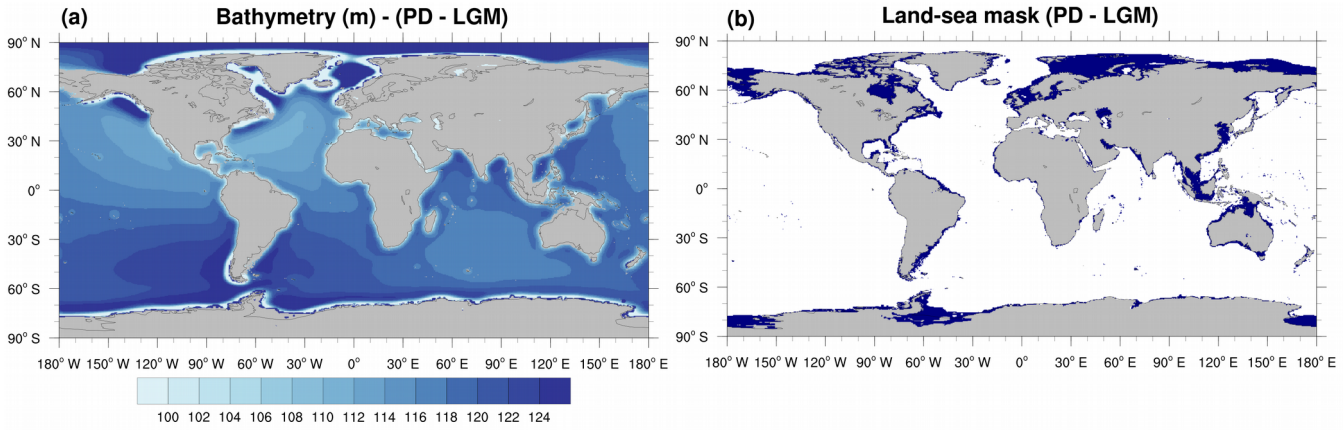

Figure 1. Difference in (a) ocean bottom depth (m) and (b) land-sea mask between present-day conditions (PD) and 21 ka BP (LGM) estimated from the ICE-6G_C ice-sheets reconstructions. Blue in (b) represents ocean area during PD that were land during the LGM.

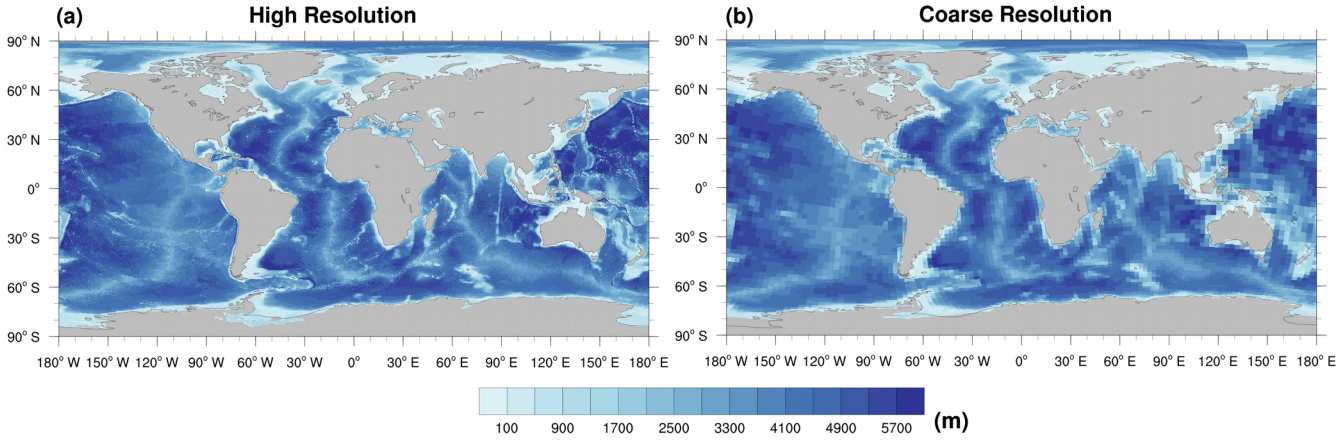

Figure 2: Present-day global ocean bathymetry (m) and land-sea mask for (a) the high resolution (HR, 10' × 10') dataset; and (b) the generated coarse resolution (GR30) grid for running MPIOM.

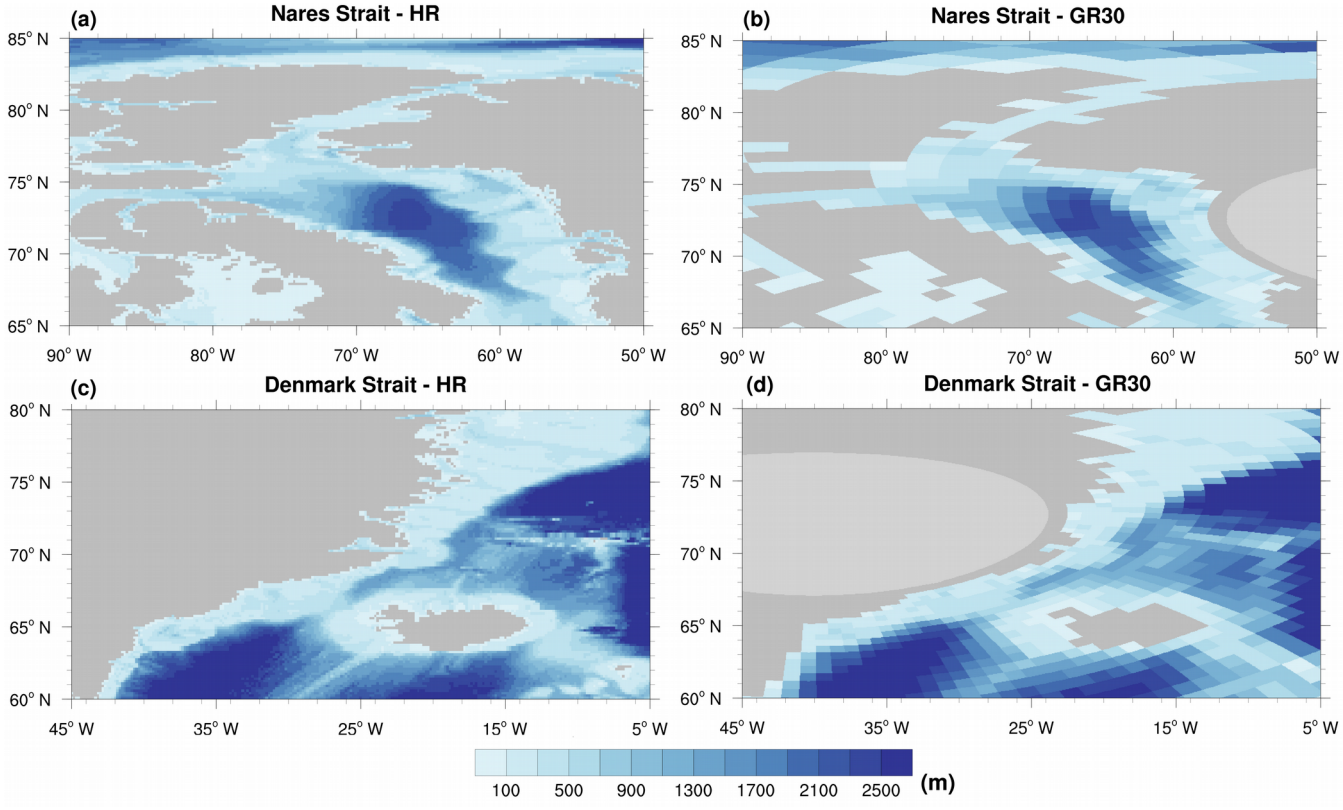

680 **Figure 3: Detailed present-day ocean bathymetry (m) and land-sea mask for the Nares Strait (a) HR; (b) GR30 and Denmark Strait (c) HR; (d) GR30.**

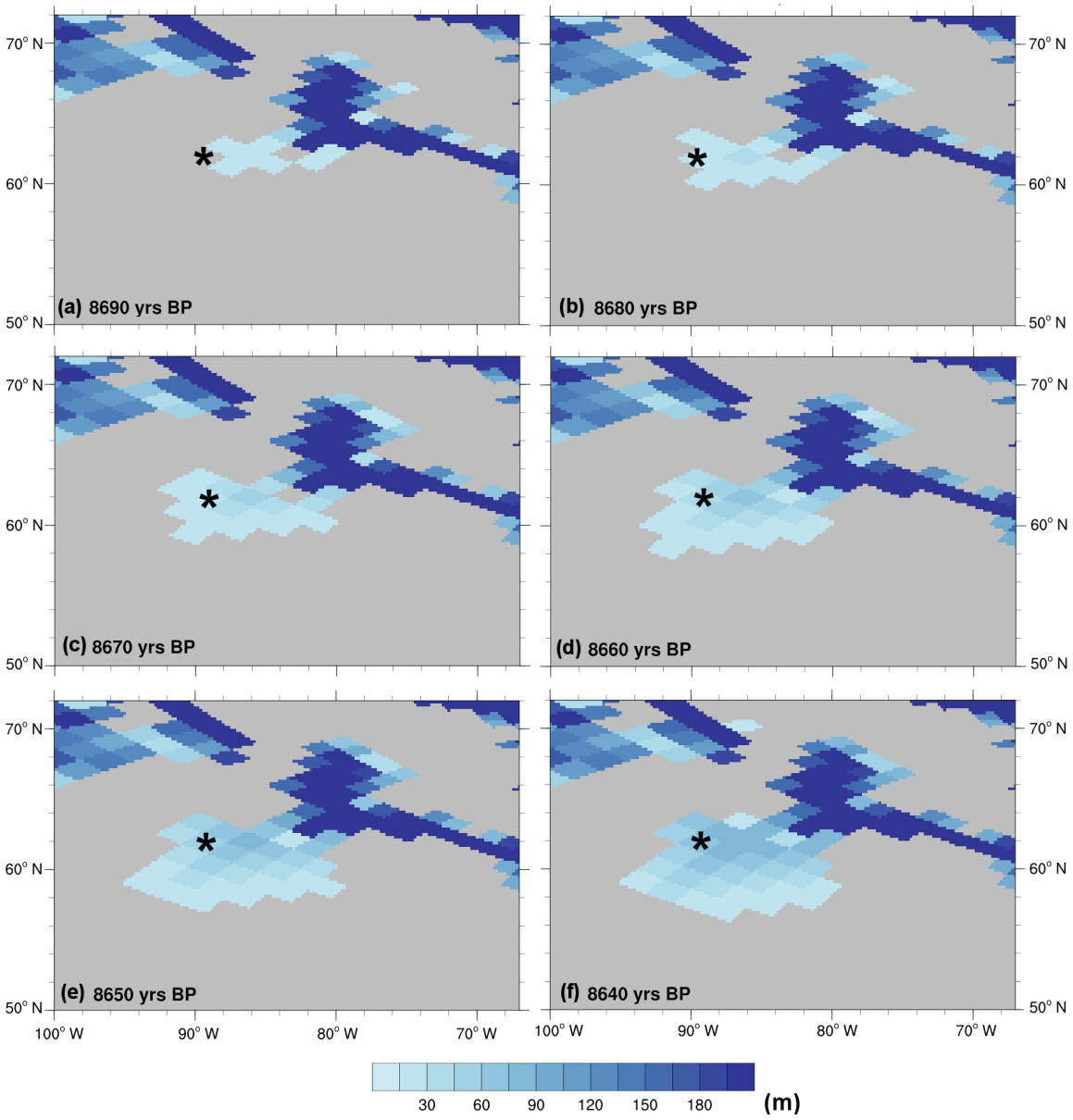

685 **Figure 4: Bathymetry fields around the Hudson Bay for different time slices (10 yrs time step) showing a gradual opening and deepening of the area. Black stars highlight a grid point as a reference.**

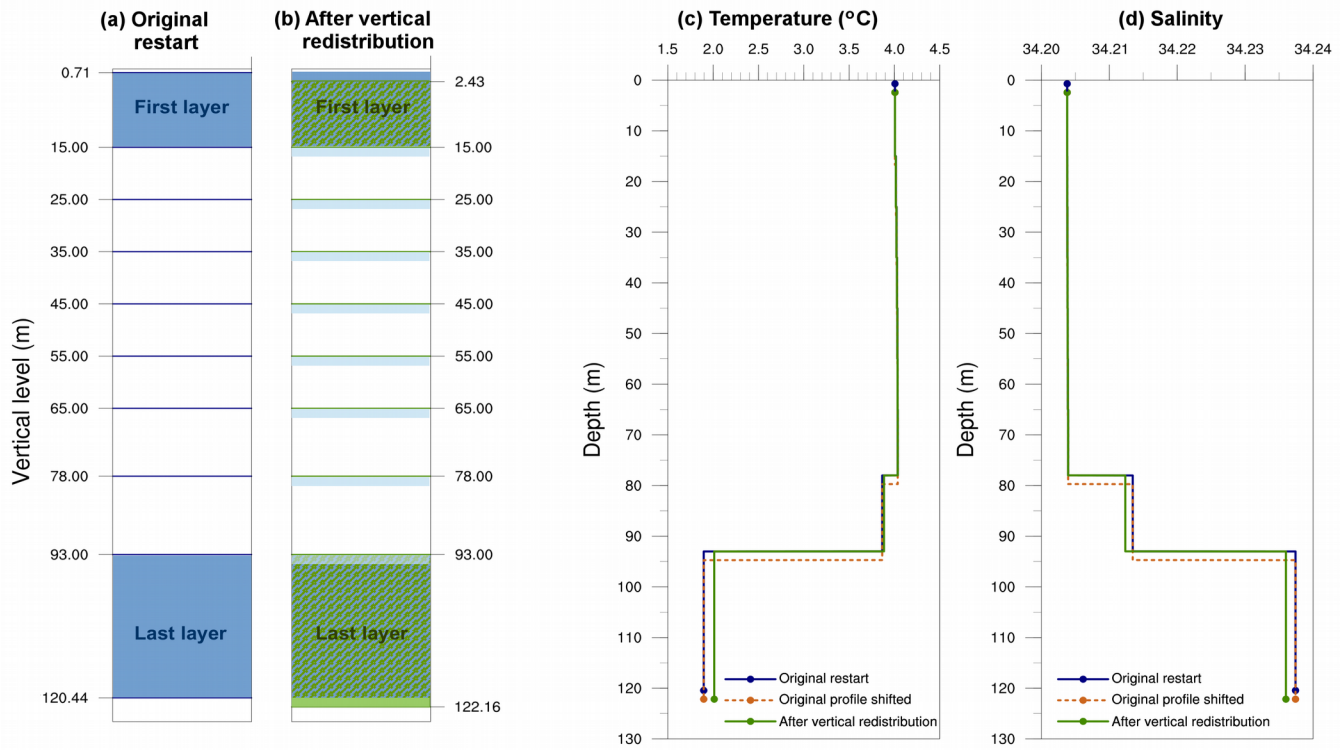

~~Figure 5: Example of the adaptation of the SSH field in order to conserve mass after changing the bathymetry. SSH field (m) (a) from the original restart file generated by MPIOM; (b) after the vertical re-location; (c) after the horizontal re-location; and (d) after performing the horizontal smoothing. Grid points coloured in yellow and pink in (c) represent a new wet and dry point, respectively.~~

~~Figure 6: Time series of relative change (%) with respect to the initial value for the computed yearly mean of (a) ocean volume; and (b) ocean surface area during the test run with MPI-ESM.~~

Figure 5: Example of vertical redistribution of water and tracers for a single wet grid point. Resulting vertical level configuration (a) before and (b) after changing the bathymetry. Blue and green areas represent the first and last vertical layer thicknesses from the original restart file and after the vertical redistribution, respectively. Hatched areas in (b) represent common thickness layer for both configurations. The light blue bars indicate where, after the vertical shift of the original profile, water from the layer above is added. Vertical profiles of (c) temperature and (d) salinity for the original restart fields (blue), the original profiles shifted downward according to the deepening in bathymetry (orange), and after applying the vertical redistribution in which the profiles are adapted to the model layers (green). Because values of tracers are constant within a model layer, the resulting profiles are stepped. Dots in (c) and (d) represent the upper limit of the first and the lower limit of the last vertical layer.

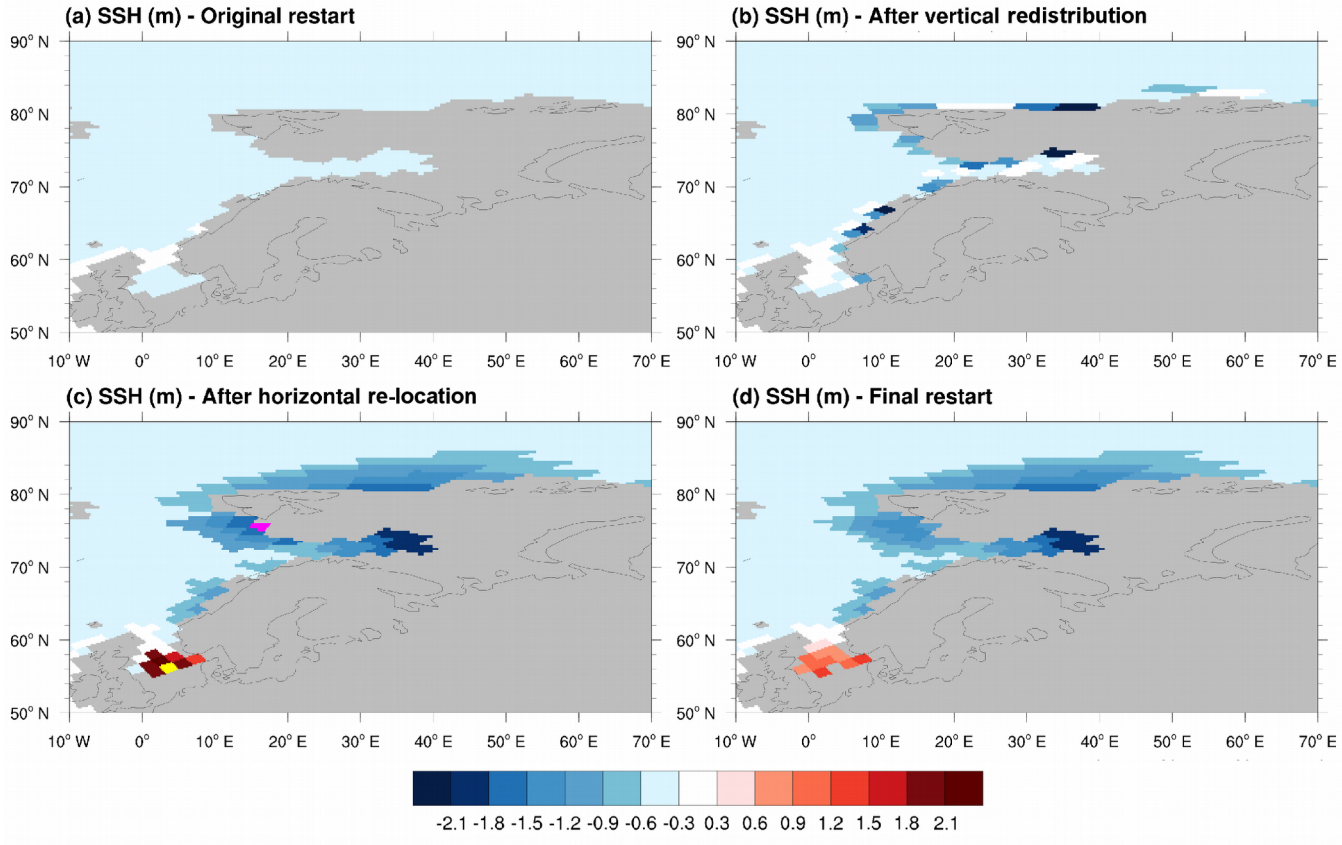

Figure 6: Example of the adaptation of the SSH field in order to conserve mass after changing the bathymetry. SSH field (m) (a) from the original restart file generated by MPIOM; (b) after the vertical redistribution; (c) after the horizontal re-location; and (d) after performing the horizontal smoothing. Grid points coloured in yellow and pink in (c) represent a new wet and dry points, respectively.

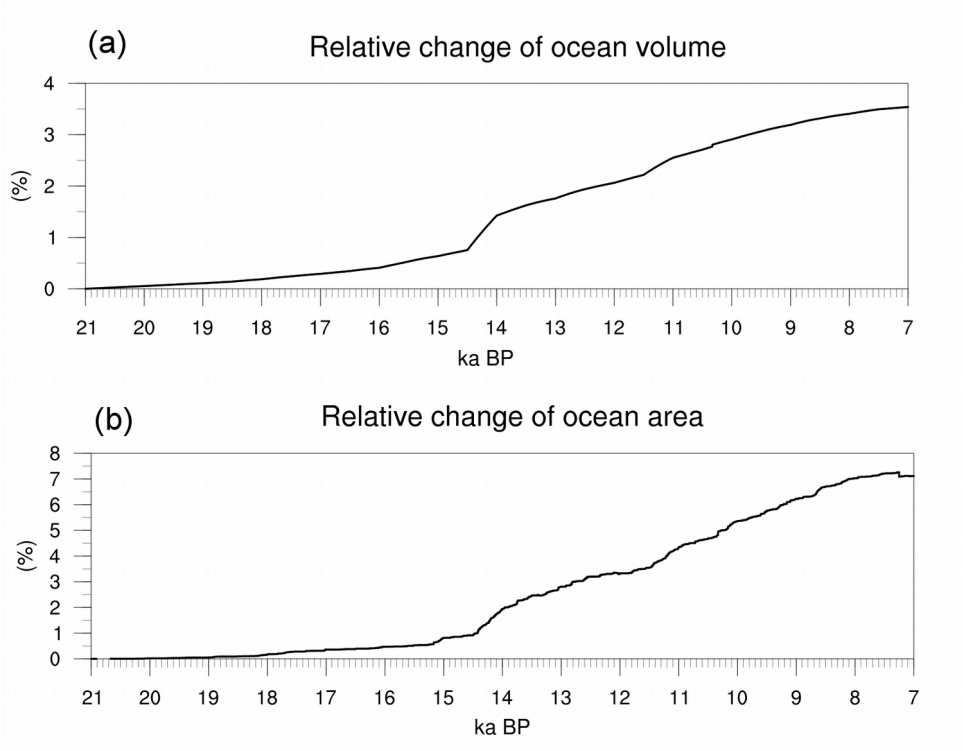

~~Figure 7: Modelled SST (°C) for (a) 21; (b) 13; (c) 10; and (d) 7 ka BP. The model can resolve the new ocean points while the ice-sheets retreat.~~

715 Figure 7: Time series of relative change (%) with respect to the initial value for the computed yearly mean of (a) ocean volume; and (b) ocean surface area during the test run with MPI-ESM.

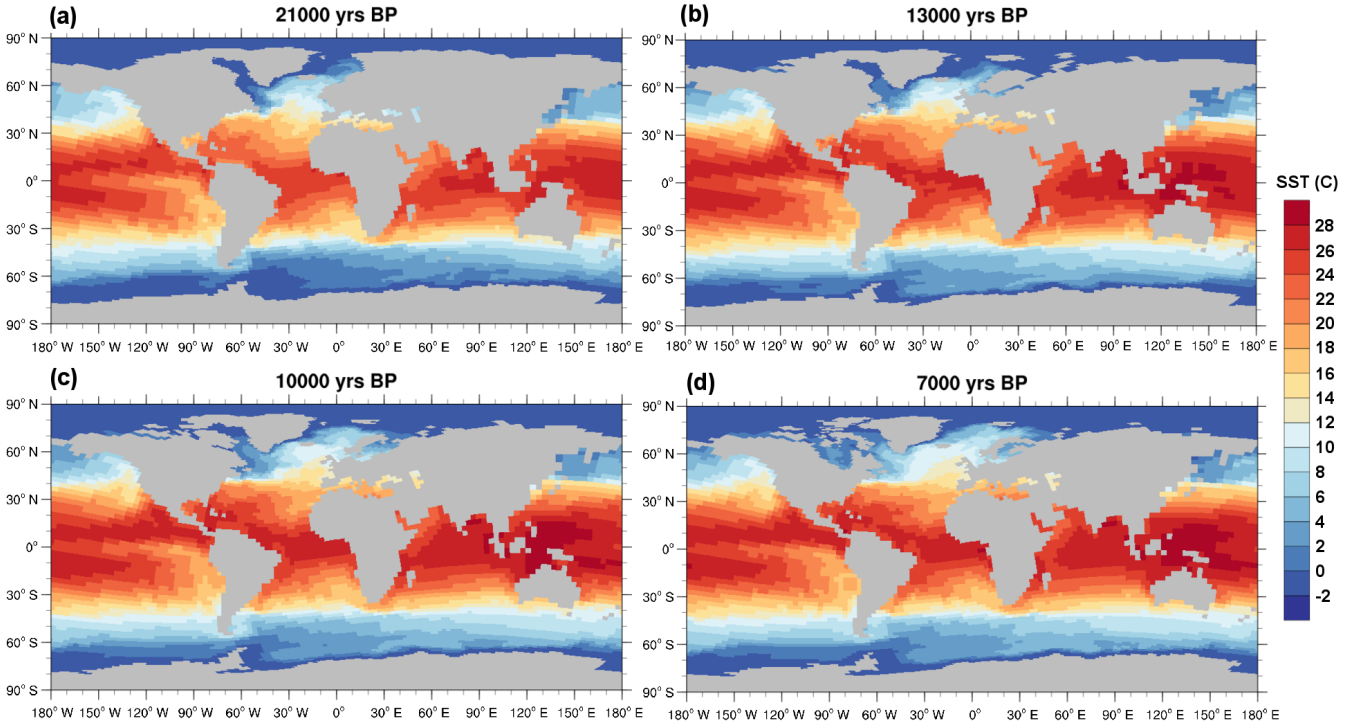

720 **Figure 8: Modelled SST (°C) for (a) 21; (b) 13; (c) 10; and (d) 7 ka BP. The model can resolve the new ocean points while the ice-sheets retreat.**

~~**Figure 8: Time series (m^3) of (a) the 10-year differences in ocean volume derived from two consecutive restart files (black line) and 10-year accumulated freshwater fluxes into the ocean (red line); and (b) difference (cm) between both divided by the ocean area during the test run with MPI-ESM.**~~

725

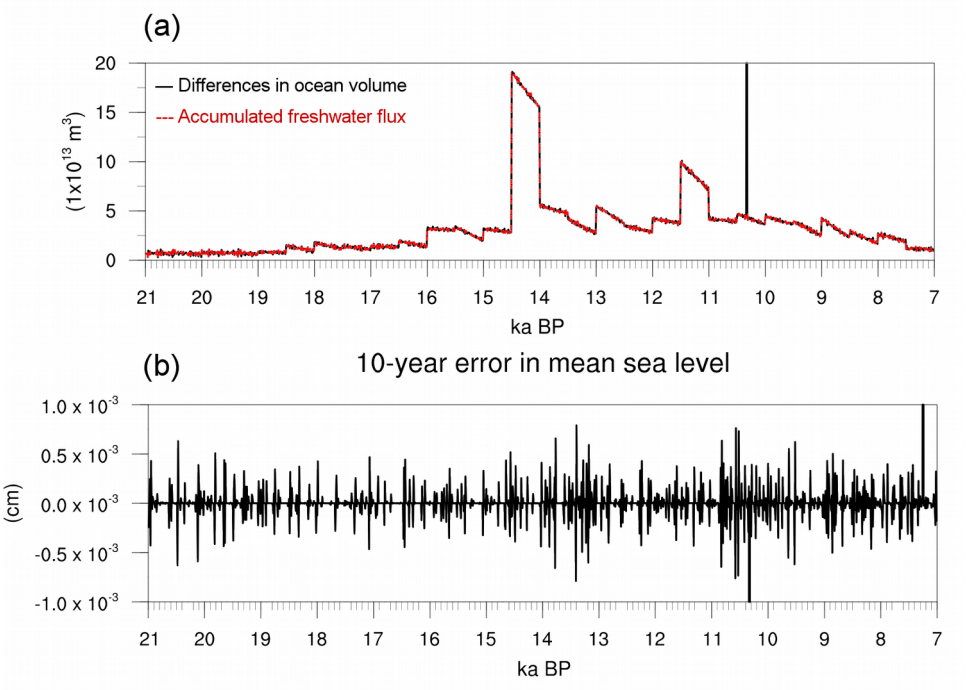

~~Figure 9: Relative change of the yearly mean global salt content during the test run with MPI-ESM.~~

Figure 9: Time series of (a) the 10-year differences in ocean volume (m^3) derived from two consecutive restart files (black line) and 10-year accumulated freshwater fluxes into the ocean (m^3, red line); and (b) difference (cm) between both divided by the ocean area during the test run with MPI-ESM.

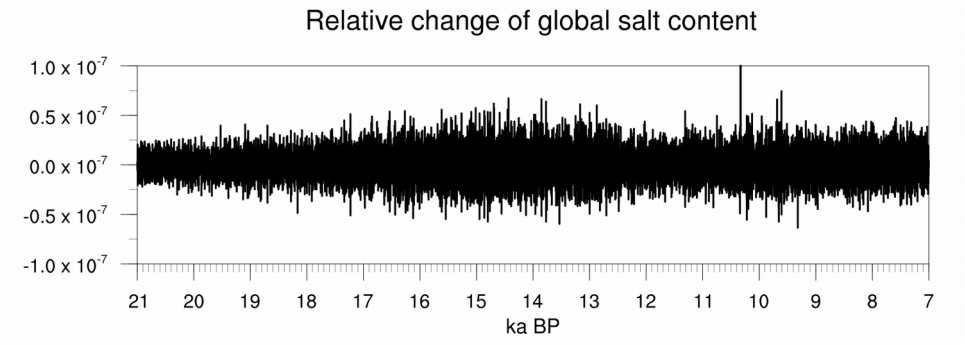

Figure 10: Relative change of the yearly mean global salt content ~~Time series of (a) 10-years instantaneous; and (b) 10-years averaged mean SSH (cm)~~ **during the test** run~~simulation~~ **with MPI-ESM.**

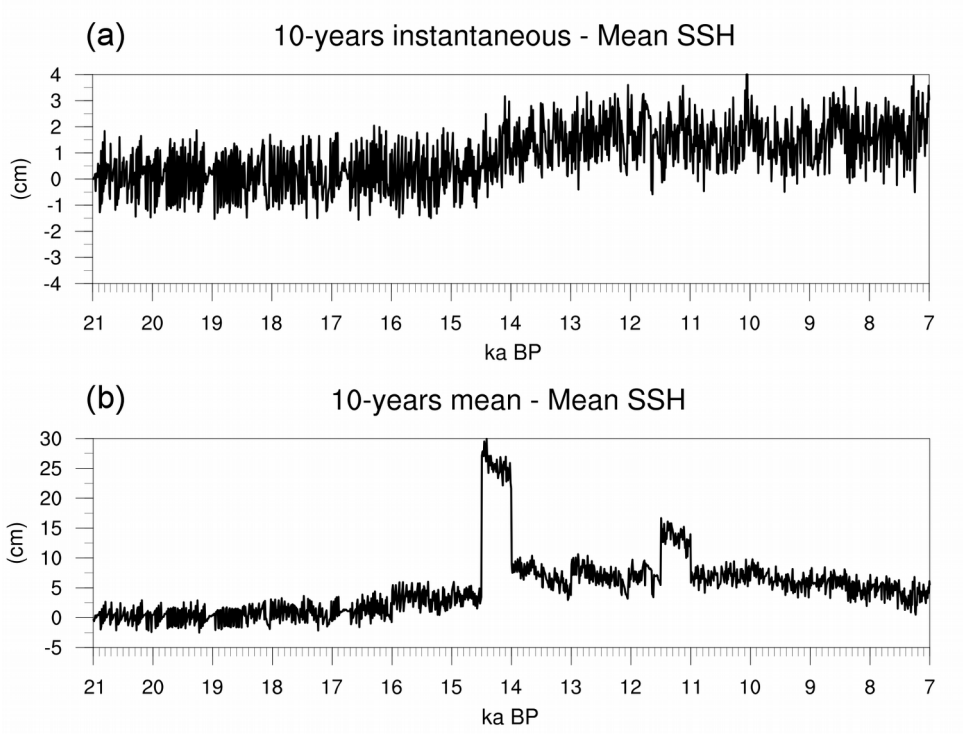

740 **Figure 11: Time series of (a) 10-years instantaneous; and (b) 10-years averaged mean SSH (cm) during the test simulation with MPI-ESM.**

Reply to Referee #1, by V.L. Meccia and U. Mikolajewicz

Review of GMD-2018-129
"Interactive ocean bathymetry and coastlines for simulating the last deglaciation with the Max Planck Institute Earth System Model (MPI-ESM-v1.2) by V. L. Meccia and U. Mikolajewicz for Geosci. Model Dev. Discuss. Doi.org/10.5194/gmd-2018-129

Overall Comments:
This paper presents a complicated multi-step algorithm for automatically and successively modifying the MPI ocean model (MPIOM) bathymetry and land/ocean mask and restart input fields in a transient simulation under evolving boundary conditions such as for ice sheet growth and melt on long time scales. The set of time-stepped ICE6-G_C boundary conditions through the deglacial period are used here to demonstrate the utility and feasibility of the method. However, the ultimate goal is to be able to incorporate active solid earth and ice sheet models to drive ocean bathymetry, volume and coastline changes due to isostatic adjustments and added ice sheet meltwater fluxes that are important for simulating climate change over a glacial-interglacial cycle. This paper documents a new procedure for approaching an extremely challenging technical problem. Up to now, when ocean bathymetry or coastlines need to be changed over the course of a long transient simulation, it necessitates much human intervention and hands-on methods that may have been designed to be used once, and thus is usually done infrequently or not attempted at all. The authors have demonstrated the success and feasibility of this new procedure that can automatically be applied at run-time and updated every 10 years for the long durations needed, though it is designed to be highly specific to MPIOM's particular model grid and architecture. I recommend acceptance after some minor revisions that could help clarify the details of the procedure.

We thank Referee #1 for his/her useful comments. We give a detailed response to each issue in what follows.

Specific comments:
1) It should be mentioned in the procedural description that an important feature of the MPIOM is the employment of partial depth bottom cells, which makes their procedure possible. Models without partial bottom cells would be constrained to discrete values of bottom depth relative to the global mean sea surface (i.e., not including the sea surface height).

We include in the manuscript a section in which the model requirements are described:

" 2 Ocean model requirements
The algorithms presented in this paper are tailored for the coarse resolution setup of MPIOM but should be easily transferable to other model resolutions or other ocean models having similar assumptions and approximations. MPIOM is a free-surface ocean general circulation model with the hydrostatic and Boussinesq approximations and incompressibility is assumed. It solves the primitive equations on an Arakawa-C grid in the horizontal and a z-grid in the vertical (Maier-Reimer 1997). For freshwater, a mass-flux boundary condition is implemented. A detailed description of the model equations and its physical parametrizations is given in Marsland et al. (2003) while its performance as the ocean component of the MPI-ESM is evaluated by Jungclaus et al. (2013). MPIOM includes an embedded dynamic/thermodynamic sea-ice model (Notz et al., 2013) with a viscous-plastic rheology following Hibler (1979). Sea-ice is swimming in the water. Ice shelves are not included. In this paper,

we use the MPIOM coarse resolution configuration with a curvilinear orthogonal grid (GR30) and two poles (Haak et al., 2003), over Greenland and Antarctica. We decide to use the coarse configuration to reduce the computational time, but the algorithms presented in this paper can easily be adapted to higher resolution grids. In the vertical, the model has 40 unevenly spaced levels, ranging from 15 meters near the surface to several hundred meters in the deep ocean. Vertical discretization includes partial vertical grid cells. Therefore, at each horizontal grid point, the deepest wet cell has a thickness that is adjusted to resolve the discretized bathymetry. On the other hand, the surface layer thickness is also adjusted to account for the sea surface elevation and the sea ice/snow where appropriate."

2) Lines 107-112: This procedure omits any lakes that form other than those connected to the Caspian and Black seas. The existence of large mid-continental post-glacial lakes formed following the melt and retreat at the southern boundary of the massive Laurentide ice sheet may be important for accurately reproducing the deglacial climate state. Drainage from Lake Agassiz, for example, and the routing of this significant source of meltwater to the ocean, is often hypothesized as causing changes in the meridional overturning circulation during the deglacial period. Excluding such lakes may be necessary in this first implementation of the tool, however, I suggest including a short explanation for why this step is required in this first implementation, the potential ramification, and plans for including them in the future.

Our algorithms are applied within the ocean model and therefore they work on the ocean domain. You are right that mid-continental post-glacial lakes are important for reproducing the deglacial climate state. But, actually, this is a problem that should be treated in the land-model instead of the ocean one. As a matter of fact, including such lakes when considering changes in the routing of the meltwater to the ocean is an ongoing work (as a follow-up of Riddick et al., 2018). For the ocean model, the freshwater fluxes into the ocean is a forcing and the algorithms presented in this paper do not treat the problem of how that forcing is derived.

Because we are solving only the ocean domain, we are interested only in lakes that are connected to the ocean, that is the Black Sea. The Caspian Sea is, indeed, an exemption because it is not connected to the oceans. However, the Caspian Sea is much larger than the other minor lakes. We decided to include it to solve the SST there that might impact on the climate of Central Asia. Therefore, solving the SST of the Caspian Sea might be important for coupled climate models.

We clarify this issue at the beginning of section *2 (now 3) Methodology*:

"Finally, we check for the presence of lakes in the GR30 bathymetry; the Caspian Sea and the Black Sea (under LGM condition, for example) are the only cases that are permitted. Because we are dealing with an ocean model, we are interested in lakes that are connected to the ocean, that is the Black Sea. However, we include the Caspian Sea in our calculations because of its potential impact on the climate of Central Asia. Solving the SST of the Caspian Sea, which is much larger than other minor lakes, might be important for coupled climate simulations. All other lakes need to be removed from the ocean domain either by connecting them to the open ocean or by considering them as land. The atmospheric model component allows accounting for lakes on land (only the thermal component). In the framework of our model system, the adequate place to calculate water storage in lakes is the hydrological discharge model."

3) As discussed again below, I found section 2.4, which describes the method for

redistributing mass and tracers vertically and horizontally in the process of adjusting the restart files, difficult to follow. For example, what is meant by "vertical re-location" in line 259. A schematic diagram depicting the procedure following changes in depth would help to clarify this procedure.

Thanks for this comment. We realize that we were not clear enough and we reformulate part of section *2.4 (now 3.4) Adaptation of the restart file in order to conserve mass and tracers*:

"Our approach consists of the following steps:

(a) Vertical redistribution of water and tracers. In this first step, we keep the land-sea mask fixed and we only deal with changes in depth. 2D fields of SSH and 3D fields of tracers are vertically adjusted to the new depth. The strategy here is to conserve the volume and amount of tracers within the water column in each grid point. Considering an individual wet point, the SSH is modified according to changes in depth in order to preserve the ocean volume locally. For example, consider a wet grid point in which the depth is 120.44 meters and the SSH from the restart file is -0.71 meters. The height of the water column results in 120.44 – 0.71 meters and the vertical levels for this configuration are shown in Fig. 5a. After changing the bathymetry, the depth at the same grid point is 122.16 meters. Because the grid area is unchanged, the SSH is lowered to -2.43 meters to conserve the volume of the water column and the vertical levels are adjusted as shown in Fig. 5b. As pointed out before, in MPIOM, the thickness of the uppermost or first layer depends on SSH, whereas the thickness of the deepest or last wet cell is adjusted to the bathymetry. The vertical distribution of tracers is consistently moved along the vertical, taking into account the new layers thickness, in order to preserve the total amount of them within the water column. The behaviour of the algorithms is displayed in Fig. 5 which shows an example of vertical profiles of temperature (Fig. 5c) and salinity (Fig. 5d). This way, the vertical profiles displayed in blue (Fig. 5c and d) are the ones from the original restart. The orange lines (Fig 5c and d) represent the original profiles shifted downward according to the change in depth. The resulting profiles after redistributing vertically the tracers to the new layer's thicknesses are displayed in green (Fig. 5d and d). Values of tracers are constant within each vertical layer of the model (stepped profile). As a result of deepening the bathymetry, the thickness of the bottom (surface) layer increase (decrease), whereas the middle layers remain unchanged (Figs. 5a and b). Therefore, to conserve tracers along the water column, vertical profiles are modified.

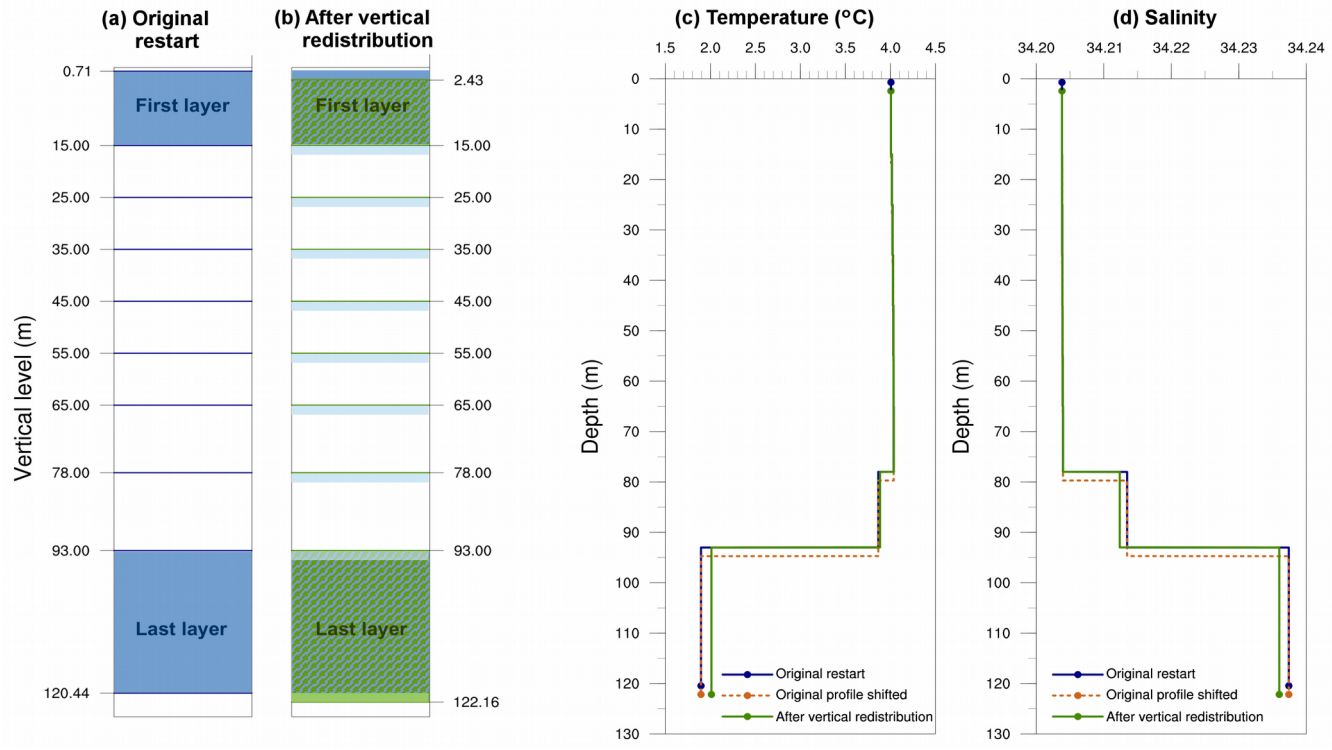

Figure 5: Example of vertical redistribution of water and tracers for a single wet grid point. Resulting vertical level configuration (a) before and (b) after changing the bathymetry. Blue and green areas represent the first and last vertical layer thicknesses from the original restart file and after the vertical redistribution, respectively. Hatched areas in (b) represent common thickness layer for both configurations. The light blue bars indicate where, after the vertical shift of the original profile, water from the layer above is added. Vertical profiles of (c) temperature and (d) salinity for the original restart fields (blue), the original profiles shifted downward according to the deepening in bathymetry (orange), and after applying the vertical redistribution in which the profiles are adapted to the model layers (green). Because values of tracers are constant within a model layer, the resulting profiles are stepped. Dots in (c) and (d) represent the upper limit of the first and the lower limit of the last vertical layer.

(b) Horizontal smoothing. The previous step is applied to each wet grid point independently, considering only changes in depth. Therefore, the resulting SSH field might present large gradients between adjacent grid points. To fix this, the SSH field is smoothed by taking into consideration the conservation of mass and tracers. That is, when necessary, values of SSH are modified by moving a volume of water with its tracer properties between adjacent ocean grid points. The maximum permitted horizontal SSH gradient between neighbouring points is set to 0.2 meters, which seems to ensure numerical stability in the ocean model.

(c) Horizontal re-location of water, tracers, sea ice and snow on sea ice when the land-sea mask changes. In step (a) we describe the procedure for dealing with changes in depth only. In this step, the new wet (dry) points resulting from changes in the land-sea mask are filled (emptied). We avoid performing any kind of interpolation in this stage because it would not account for conservation of mass and tracers. Instead, in order to conserve properties, the necessary amount of water and tracers to fill new wet points is taken from other boxes. The simplest approach would be to take water from all ocean boxes. However, this would involve the artificial long-distance transfer of water mass properties.

Therefore, we decide to use only adjacent ocean boxes. That is, small volumes of water with its properties coming from adjacent points is placed into the new wet point until completely filling it. Similarly, the amount of water and tracers from a point which is dried is re-located among the neighbouring wet grid points. This operation is repeated for sea ice and snow on sea ice. There needs to be a compromise between involving only a few neighbouring grid points and the risk of obtaining large horizontal gradients of SSH. Sensitivity tests were performed to achieve the optimal balance for both, filling and emptying procedures.

(d) Horizontal smoothing. Again, we apply step (b) to obtain a sufficiently smooth SSH field to ensure numerical stability when running the model."

Thus, a figure was added to the revised manuscript and figure numbering has changed accordingly.

4) There is no mention of what is done to adjust velocity components and other related fields that restart the flow fields following changes in land/ocean mask and bathymetry.

The aim of adapting the restart file when bathymetry and land-sea mask change is to account for the conservation of mass and tracers. Therefore, the modification of the fields is done for sea surface height, sea-ice, snow on sea ice (because they are key variables for the total ocean mass), temperature, salinity and passive tracers (because we want to conserve tracers). We do not perform any computation for the other variables (including velocity components) and, therefore, their values remain unmodified. Thus, when wetting a new grid point, the values of the restart file for velocity, for example, will be zero because it is the value for a dry/land point. During the restart procedure MPIOM anyway guarantees that velocity on land points is set to zero. Considering the horizontal resolution that is currently being applied in long simulations with climate models, the advection of momentum is of minor importance. Far from the equator, velocity can be approximated pretty well by frictional geostrophy, as done in the LSG model (Maier-Reimer et al., 1993). Even though velocity is formally a prognostic variable of the ocean model, it is de facto a diagnostic variable whereas the main prognostic ones are temperature and salinity and sea ice. This fact is exploited in typical set-up procedures, where the ocean is initialized with fields of temperature and salinity (from climatology or other model runs) and at rest. However, after one month the velocity field is adapted to the hydrographic fields.

We mention that in section *2.4 (now 3.4) Adaptation of the restart file in order to conserve mass and tracers*:

"The last modelled state of the ocean with its ocean configuration (restart file) will be used as the initial state for the later setup. Hence, the 2D and 3D fields should be adapted to the new bathymetry and land-sea mask. When carrying out this task, our aim is to account for the conservation of mass and tracers not only at global but also at regional scale. Therefore, the variables that are adapted in this step are SSH, sea-ice, snow on sea ice (for conserving mass) and tracers (for conserving them). From here on, when referring to tracers, we mean temperature, salinity and any passive tracer that MPIOM prognostically resolves (age tracer, radioactive tracer, CFC, etc.). The other model variables (like for example velocities) are not being modified. During the restart process, MPIOM multiplies the velocities with the land-sea mask, thus non-zero velocities are not a problem. However, on the coarse horizontal resolution applied in these very long climate model simulations, the velocities in the ocean are determined essentially by geostrophy and friction and after one month of simulation, the velocity field has adapted to the hydrographic fields. Our approach consists of the following steps:"

5) Section 3 describes how freshwater fluxes are added to the ocean from the melt of

grounded ice sheets by the river discharge model, effectively increasing ocean volume. Section 2 describes the procedure for changing bathymetry and ocean volume using the ICE6-G_C data, implicitly changing volume due to melting ice sheets. Figure 8 shows the procedure works out as the volume change from these two processes match, but it reads like the ocean volume is being changed twice here. Is it because the bathymetry changes are made as a result of the meltwater added slowly over previous interval of time (10 years) since last bathymetric changes? Thus, new volume, added through bathymetry changes, lags or catches up to the volume change due to freshwater added through meltwater over the preceding interval? A schematic showing all of these complicated steps would help clarify.

Ocean volume is not being changed twice. Section 3 describes the transient simulation we performed in order to test the algorithms. The ICE6-G_C reconstructions were used to derive the HR topography and to compute the time-dependent freshwater fluxes into the ocean as in eq. (4). This step is necessary here because the HR topography is prescribed in this experiment and will not be needed when coupling the climate model with the ice-sheet and solid earth models. The ice-sheet growth or decay and the resulting net freshwater flux into the ocean is the only responsible process for the changes in ocean volume and ocean surface area (fig. 6). Therefore, the changes in ocean volume should match the net freshwater fluxes into the ocean (fig. 8), except for the delay caused by the time needed within the hydrological discharge model to transport the water to the ocean.

When running the model for 10 years with a fixed bathymetry, the imbalance of net freshwater fluxes into the ocean affects the mean SSH, which is simply a consequence that during the 10 year simulation the ocean volume has changed and is not matching exactly the bathymetry any more. After 10 years, the bathymetry and land-sea mask change and the mass of water is distributed to the new configuration. This way, the mean SSH is being preserved within the simulation. This would work perfectly if a) the model ocean bathymetry had the same horizontal resolution than the topography used to compute the freshwater fluxes into the ocean; b) the data used for computing the freshwater fluxes and HR topography was consistent because it accounts for conservation of water. However, a) reducing the resolution from HR to GR30 results in a smoother bathymetry that might result in differences in ocean volume (between the one that would be for HR and the one that results for GR30); b) we aim at writing an algorithm independently of the data used as forcing and so we consider the potential inconsistencies in the reconstructions. Hence, the aim of step 2.3 is to correct these two possible sources of inconsistencies. The strategy is to match the last ocean volume state (GR30, which already accounts for the accumulated freshwater fluxes during the previous 10 years) with the ocean volume of the new configuration (GR30 that might contain artificial changes in ocean volume due to the loss of bathymetric details when reducing resolution and to potential inconsistencies in the HR topography). The resulting ocean GR30 bathymetry accounts for changes in the ocean volume only due to the imbalanced net freshwater fluxes.

We understand that this issue is not clear enough in the original manuscript and we modify section *2.3 (now 3.3) Matching changes in ocean volume and freshwater fluxes into the ocean*:

"The growth or decay of ice sheets and the resulting net freshwater flux into the ocean is the only responsible mechanism to change the volume of the ocean in MPIOM, as incompressibility is assumed. Otherwise, effects like thermal expansion could be important as well. When running the model with a fixed bathymetry, the net freshwater fluxes into the ocean affect the mean SSH and consequently the thickness of the uppermost ocean layer. When a new ocean bathymetry is derived in a formally independent process, the mass of water is distributed to the new configuration. Then, both estimates of

the ocean volume should be consistent, and therefore, the mean SSH and mean thickness of the surface layer should be preserved within the simulation for all restart points. However, de facto, this is not always the case mainly for two reasons. On the one hand, the HR reconstructions might show inconsistencies if they do not account for water conservation. On the other hand, reducing the resolution from HR to GR30 can cause disagreements in the ocean volume due to the loss of details in the bathymetry field. The aim of this step is to remove these two possible sources of inconsistencies. The procedure is to match the last GR30 ocean volume, which already accounts for the freshwater fluxes into the ocean, with the ocean volume of the new GR30 configuration, by performing the following steps:"

and later in the same section:

"In this way, the resulting ocean GR30 bathymetry accounts for changes in the ocean volume due only to the freshwater fluxes into the ocean. There might exist slight discrepancies produced by the last step. However, by removing possible artificial changes in ocean volume, the procedure ensures that the mean SSH is reasonably well preserved, independently of the freshwater fluxes and the prescribed HR dataset."

Minor comments by line:
63: "In the frame of the project..." -- awkward phrase to start the sentence.

Reformulated to:

"Our long-term goal in the context of the project "From the Last Interglacial to the Anthropocene: Modeling a Complete Glacial Cycle – (PalMod)", is to simulate the last termination with a coupled ice sheet-solid earth-climate model with interactive coastlines and topography forced only with solar insolation and greenhouse gases concentration."

150: OK--omitting Arctic and Southern Oceans in this list because they are contiguous with the other major ocean basins?

Yes. Atlantic-Pacific-Indian Oceans was changed to World Oceans:

"The strategy is to keep only the wet points that are directly connected to one of the following basins: World Oceans, Mediterranean Sea, Red Sea, Black Sea and Caspian Sea."

Accordingly, it also was changed in line 163 of the original manuscript.

171:"Specific regions are examined in detail and modified if necessary." Also, "...look at the HR land-sea mask..." Suggests human oversight here, but I suspect this is not the case. This step must use some rather specialized coding because many specific regions in the HR mask are checked against the new GR30 mask. What methods are used to make this more automatic? Are multiple solutions possible to obtain using the fraction ocean in the new GR30 to identify pathways that connect new regions?

Yes, this step is done automatically by the code. We explain it in the revised manuscript:

"Specific regions are considered in detail for further checking and the GR30 land-sea mask is, therefore, modified if necessary. First, we check if North and South America are connected by land or

artificially separated by the remapping. Then, we check some straits or channels (Strait of Gibraltar, Bab-el-Mandeb, Bosphorus, Denmark Strait, Faroe-Shetland Channel, Northwest Passage, Nares Strait and the Strait of Sicily), islands (Indonesia and Japan) and peninsulas (Florida, Thailand-Malaysia, Kamchatka, Italy and the Scandinavian Peninsula). The strategy here is to automatically control if the straits/channels are open or closed and if the islands/peninsulas are isolated from or connected to the mainland in the HR land-sea mask. To automatically perform this task, the algorithm finds the path of connection between two points apart. This is done in a restricted domain around the region of interest. For example, when checking the opening or closure of a strait, the points to be connected are wet points located in each side of the strait. If the algorithm finds that the path of connection between both points is always within the ocean, that means that the strait is open. Instead, if the path of connection is blocked by land, that means that the strait is closed. The location of each pair of points was manually and carefully decided for each region and is fixed in the code. It was tested that those points do not change from wet to dry or vice versa during the last deglaciation. The approach is applied to each specific region mentioned before and both resolutions, HR and GR30. When necessary, the GR30 land-sea mask is regionally modified to be consistent with the HR data. The information of the fraction ocean is used to decide about the path of the opening or closure. Being the fraction ocean a float number it is highly unlikely to obtain multiple solutions. In that case, the algorithm would choose the first solution found."

Section 2.3 and section 3, lines 300-308: Globally adjusting ocean depth to keep global mean SSH constant, and volume changes through adding freshwater from melting ice sheets. Are the steps employed in Section 2.3, done every timestep after freshwater from melting grounded ice sheets is added, thus increasing global ocean volume through increases in SSH?

In the transient simulation we performed, the freshwater fluxes into the ocean are being incorporated every time step, whereas the procedure described in section 2.3 is being applied only for constructing a new ocean bathymetry, in this case, every 10 years. We clarify this aspect in the revised manuscript. Please, see the answer to your point 5) of "*Specific comments*" for more details.

248: Do the final changes made to depth as described in step 2.3(d) require iterations back to (3)?

No. It is important for the model stability that the final depth satisfies eq. (2). For example, a new wet point must have a depth smaller than the thickness of the surface layer in the model. This is to avoid involving more than one layer when adapting the restart file. Going back to this criteria might destroy some corrections done in step 2.3 (now 3.3) as stated in the manuscript:

"In this way, the resulting ocean GR30 bathymetry accounts for changes in the ocean volume due only to the freshwater fluxes into the ocean. There might exist slight discrepancies produced by the last step. However, by removing possible artificial changes in ocean volume, the procedure ensures that the mean SSH is reasonably well preserved, independently of the freshwater fluxes and the prescribed HR dataset."

Yet, we demonstrated that water is being conserved in a long-term transient simulation (fig. 8) indicating that, if the discrepancies still exist, they are not large enough to affect the mass conservation.

259: Section 2.4(a) What is meant by "vertical re-location"? I find this section difficult to

understand the actual details of the method even after looking at Figure 5. A schematic illustrating the method would be helpful, especially for locations that are already "wet" point that become deeper. How are tracers at mid-depth changed? Also does the process of vertical re-location" result in lateral gradients at depth in the ocean, even after horizontal smoothing? 263: "new layer's thickness"?

We better explained the methods and we added a new figure in the revised manuscript. Please, see the answer to your point 3) of "*Specific comments*" for more details.

300: The "instantaneous time derivative of the gridded ice thickness" is computed for the meltwater fluxes added by the hydrological discharge model. Does this gridded ice sheet thickness come from the ICE6-G_C data interpolated in time to every 10 years? Does "instantaneously" mean the meltwater flux calculation is done every time step, or for every 10-year interval?

Yes, the gridded ice sheet thickness comes from the interpolation in time to every 10 years. The derivative is done once for every 10 years interval. We clarify this in the revised manuscript:

"The interpolated ICE6-G_C reconstructions were also used to compute the time-dependent freshwater fluxes into the ocean. First, the 10-year interval time derivative of the gridded ice thickness is calculated. Only the ice-sheet thicknesses at grounded points are considered. The time rate of change of this quantity is then divided by the density ratio between ice and freshwater to obtain the extra freshwater flux into the ocean:
eq. (4)
where *Ice* is the ice thickness of the grounded-ice sheets and *R* the density ratio between ice and freshwater. The resulting value is considered constant for a period of 10 years, although it is introduced to the model every time step. The extra freshwater is transported into the ocean through a hydrological discharge (HD) model which considers the changes in river routing (Riddick et al., 2018)."

366: "...called with a maximum of three input files." The description of the tool software and scripts is short. A bit more information about how it is used in practice and integrated into the model run-time would be helpful. For example, how does it interface with the model during run-time? Which input files are needed? Is the tool launched in the main run script, at the start of a restart submission using files from the previous submission? Because restart files are generated, does this mean that the 10 year time interval between bathymetry changes fixes the maximum number of years between resubmission?

A more detailed description is included in the revised manuscript:

"The principal tool consists of shell scripts that are called with a maximum of three input files. All the calculations are performed with CDO commands and programs written in FORTRAN. The tool can easily be included at the end of the main run script without the necessity of interrupting the simulation. There are two shell scripts that need to be called after the restart file is written by the model. The first one generates the new bathymetry file for running MPIOM. Two input files are required to run this script. The first one corresponds to a NetCDF file containing the new HR bathymetry. The second input is an ASCII file which corresponds to the previous GR30 bathymetry as it was read by MPIOM. The output of this shell script is an ASCII file containing the new GR30 bathymetry to be read by the model. As a result, this script replaces the old bathymetry file to run MPIOM with the new one. The second shell script adapts the restart file generated by the model to the new ocean configuration. This

script needs three input files. The first and second ones correspond to the old and new bathymetry files as read by MPIOM, respectively. The last input is the restart file generated by the model in NetCDF format. The output is the modified restart file in NetCDF format to replace the original one. The execution of this tool needs the restart file generated by the model as input. Therefore, it can be called only after a restart file is generated. Contrary, it is possible to resubmit the job without applying the tool, that is with fixed bathymetry, land-sea mask and, therefore, unmodified restart file. This allows for a shorter number of years between resubmissions than the ones required for changing the bathymetry. Consequently, the tool is easy to apply and it is fast, taking less than a minute to run on a workstation."

Reply to Referee #2, by V.L. Meccia and U. Mikolajewicz

Review of the paper entitled "Interactive ocean bathymetry and coastlines for simulating the last deglaciation with the Max Planck Institute Earth System Model (MPI-ESM-v1.2)" by Virna Loana Meccia and Uwe Mikolajewicz.

This paper has been long awaited by the community working on the last deglaciation from LGM to present day. But, in fact, this methodology could also be interesting for simulations for future deglaciations of Greenland and West Antarctica in the next century.

Indeed in the framework of PMIP4 deglaciation project (Ivanovic 2016) in which models intend to provide transient simulations from LGM to PD, such tool is absolutely needed.

The authors aim to use the MPI ESM to produce deglaciation transient runs. They cope with a long lasting issue and resolve it: how to modify boundary conditions that account for sea level rise during the deglaciation and modify the topography (bathymetry and coastal lines) all along this process using algorithms that avoid manual and more or less subjective corrections. They describe the algorithms they used for adaptation of the ocean model MPIO at low resolution used in the PMIP4 exercise with boundary conditions evolving every 10 year.

The paper is well written and its structure is clear. The detailed description of strategy target and problems is convincing.

We thank Referee #2 for his/her useful comments. We give a detailed response to each issue in what follows.

My major comments are the following:

1. the paper is perfectly suited for GMD. Nevertheless the authors never tackle the effect of their boundary condition changes on deglaciation. Therefore I suggest that they address this question at least concerning two important points

We propose this paper to GMD as a "Development and technical paper" because it presents a novel methodology consisting of several steps tackling a challenging technical problem. We believe that a detailed description of the algorithms deserves a paper itself and therefore we are submitting a purely technical paper. Thus, we are not aiming at analyzing the climate response to a changing bathymetry and land-sea mask in this study. The effects of including our algorithms in a transient simulation of the last deglaciation in terms of the climate response will be faced in another paper and it is an ongoing work.

- **Discussing the added value of this study compared to previous simulations where the bathymetry was not changed to better emphasize what may be the interest of this study beyond the technical challenges.**

  Discussing the added value of applying the algorithms described in the manuscript in comparison to a simulation in which the bathymetry and land-sea mask are fixed is for sure a very interesting and necessary issue. However, as mentioned before, it is not the aim of our manuscript and it will be the topic of another paper. We believe that the effects of including a variable topography for simulating the last deglaciation deserve a detailed study itself. Indeed,

we have run the model with the same conditions as the ones described in section 3 of the original manuscript, but with fixed bathymetry and land-sea mask to the LGM, that is, without applying the algorithms. Figure A1 shows an overview of a comparison between both simulations. As an example of some variables, we plotted time series of a) AMOC at 26N and 1000 meters depth; b) sea-ice extent in the Arctic; c) global SST and; d) global SSS for the run with variable (red) and fixed (blue) bathymetry and land-sea mask. We observe differences in the behaviour of the variables, particularly from 14 kyrs BP onward, when the ice-sheet melting rate is high and the changes in the coastline are large. Therefore, there are substantial differences between both simulations. However, a detailed study would be needed to explain the effects of applying our methodology in terms of the physical mechanisms and the climate response. We are planning to face it in another paper. In our current manuscript, instead, we intend to present the technical problem and the way we propose to solve it as a “Development and technical paper”.

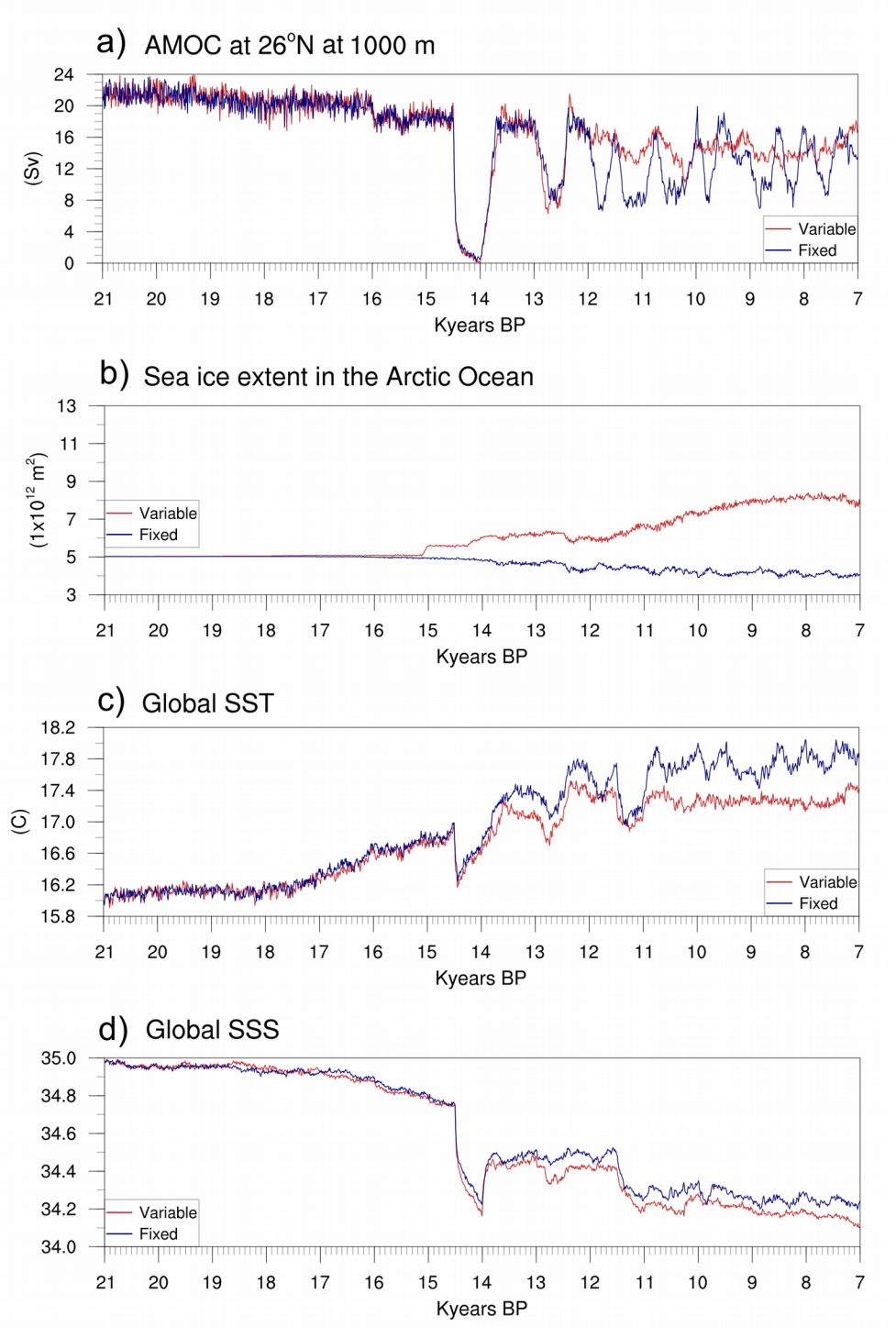

Figure A1: Time series of a) AMOC at 26N and 1000 meters depth; b) sea-ice extent in the Arctic; c) global SST and; d) global SSS for a simulation of the last deglaciation with variable (red) and fixed (blue) bathymetry and land-sea mask.

- **The authors should also emphasize the potential limitations of this method in terms of simulating abrupt events during deglaciation due to many linear processes they used, both in time and space. I perfectly understand smoothing procedures the authors described to avoid crash of the model, but during deglaciation many non linear changes occurred for**

instance MPW and more generally acceleration of melting rates described for instance in C. Waelbroeck et al., Quaternary Science Reviews 21, 295-305, 2002, for the last 30k. Therefore the authors should discuss in more details what is the compromise between avoiding crash and capturing real non linear events.

We apply our methodology to MPIOM, the ocean component of the MPI-ESM. We are not computing a variable topography in response to the melting rates and the isostatic adjustments. Instead, our algorithms read the topography fields in high resolution and construct a usable bathymetry to run the ocean model in a coarse resolution. Thus, changes in topography due to the ice-sheet growth or decay and the isostatic adjustments of the bedrock are prescribed input data for our tool. In the experiment we present in section 3 of the manuscript, we use the ICE6-G reconstructions to construct the prescribed high-resolution topography. Changes in topography can also be solved by an ice-sheet model and a solid earth model coupled to the ESM, but these changes are computed neither by the ocean model nor by our algorithms. In that sense, the abrupt events and non-linear changes in the melting rates that took place during the deglaciation are not affected by our procedure. We agree with the reviewer, that the abruptness of some of the past changes is not captured by linearly interpolating between time slices 500 years apart. We did not produce these data, so we had to work with what was available. However, we should stress, that the PMIP deglacial simulation is not the goal, but only a simple test bed. Our ultimate goal is the fully coupled model with atmosphere, ocean, ice sheets and solid earth, which automatically generates higher resolution (in time) signals.

When applying our methodology in a transient simulation, the changes in bathymetry and land-sea mask are limited for the ocean model, but those limitations are not affecting the evolution of the bottom topography due to the ice-sheet retreat. The algorithms read the high resolution topography and allow only small changes when generating the coarse resolution bathymetry to run MPIOM. This fact can slow down the flooding and drying events of the shelves regarding the ocean domain. Therefore, due to the smoothing method, the propagation of the coastline is affected. In any case, if this is a problem for the solution, the algorithms can be applied more often (every year, for example). From the results shown in section 3 of the manuscript, we conclude that changing the bathymetry every 10 years during the last deglaciation is an optimal compromise for our model setup between both, model performance and computing time. In general, the stencil for adaptation could be widened, which would allow a faster flooding of e.g. the Hudson Bay. This might be necessary also when using a model with higher horizontal resolution.

We clarify this point in section *4 Remarks*:

“There are mainly three limitations in our technique. First, the fact that changes in depth and coastlines are limited can slow down the flooding and drying events of the shelves. However, it is important to note that changes in topography in response to the ice-sheet retreat and isostatic adjustments are solved neither by the ocean model MPIOM nor by our algorithms. Instead, the HR topography is prescribed to our tool or solved by the ice-sheet model. In this sense, the non-linear changes or abrupt events that occurred during the last deglaciation are not affected by our methodology. Still, if the timing of the flooding and drying events of the shelves is considered to be critical, the algorithms could be applied more often within the simulation (every year, for example). However, in MPI-ESM, changing the topography implies also changes in the river routing and the land mask for the atmospheric model. Therefore, there should be a compromise between the frequency that topography is being changed and the computational time. From our

results, we conclude that changing the bathymetry every 10 years during the last deglaciation is an optimal compromise between both, model performance and computing time. Another possibility would be to widen the stencil used for collecting water for new ocean points. This would allow a faster propagation of coastlines by more than one grid point per iteration. This might also turn out to be necessary when applying the tool to ocean configurations with higher horizontal resolution."

2. The authors should also clarify the part of the paper that may be directly useful for the PMIP4 deglaciation community and those that have been developed specifically for MPI ESM.

We include it in section *4 Remarks:*

"Second, this tool was originally written for the curvilinear orthogonal grid (GR) with two poles. Although we presented in this paper the results for the coarse resolution GR30, the tool can be also applied for the low resolution (GR15) configuration of MPIOM. Still, for the moment its usage is limited to GR grids. We are currently working on a new version to include the tripolar (TP) quasi-isotropic grid (Murray, 1996) among the applications. In general, the algorithms are easily adapted to any ocean model that meets the same requirements as MPIOM: Arakawa-C grid in the horizontal, z-grid in the vertical including partial bottom cells, free-surface and mass flux boundary conditions. However, there are some parameters inside the scripts that depend on the grid. They are the location of each pair of points in order to perform the checking steps described in Sect. 2.1 for correcting the bathymetric details."

Whereas this paper is worth to be published in GMD, I have also minor comments that it would be important the authors answer to before publication.

Minor comments:

Abstract:

A1 What do the authors mean by conservation of mass and tracers at regional scale. It is a bit misleading in the abstract. I think the authors have in mind to keep regional conservation when changing spatial resolution. They should clarify this issue.

If some correction is needed to globally conserve mass and tracers, it is enough to distribute homogeneously a single value around the globe. By conserving mass and tracers at a regional scale, we mean that changes in a single grid point are not propagated globally. In other words, we avoid propagating water properties over long distances by affecting only regionally the potential changes in a single grid point.

We clarify this point in the *Abstract*:

"The strategy applied is described in detail and the algorithms are tested in a long-term simulation demonstrating the reliable behaviour. Our approach guarantees the conservation of mass and tracers at global and regional scales, that is, changes in a single grid point are only propagated regionally."

A2 The authors, first tackle a very general problem: the bathymetry adaptation when simulating the last deglaciation. How far the algorithm developed here, beyond grid specificity can be easily

adapted to other models. A sentence in the abstract should clarify this point.

We add a sentence in the *Abstract*:

"For the first time, we present a tool allowing for an automatic computation of bathymetry and land-sea mask changes in the Max Planck Institute Earth System Model (MPI-ESM). The algorithms developed in this paper can easily be adapted to any free-surface ocean model that uses Arakawa-C grid in the horizontal and z-grid in the vertical including partial bottom cells. The strategy applied is described in detail and the algorithms are tested in a long-term simulation demonstrating the reliable behaviour."

Introduction:

I1 The first sentence is very general and partially untrue because of some aspects of the unprecedented speed of ongoing climate change. The authors should remove or modify this sentence.

The sentence is removed:

"During the last deglaciation, the Earth transitioned from the last glacial to the present interglacial climate, experiencing a series of abrupt changes on decadal to millennium timescales."

I2 The authors should mention that major uncertainties remain on reconstruction of Antarctica at LGM. Indeed, NH ice sheet reconstructions are better constrained, whereas Antarctica ice sheet reconstruction has often been an adjustable parameter. Therefore, the authors should mention Antarctica reconstruction uncertainties at LGM both from data and models (G. Philippon, Earth and Planetary Science Letters 248 (2006) 750.)

The quality of the reconstructions is not the point of our paper. Our algorithms are applied to the ocean model and they do not care about the prescribed topography. Therefore, the tool we are presenting is independent of the uncertainties on reconstructions. We are using ICE6-G in our transient simulation just as a test case. We could also use Tarasov or even the modelled topography from the coupled ice sheet solid earth model PISM/VILMA as it is planned for the future. Anyway, we mention it in *1 Introduction*:

"Differences in ocean bathymetry and land-sea mask between present-day conditions and 21 ka BP calculated from the ICE-6G_C ice-sheets reconstructions (Argus et al., 2014; Peltier et al., 2015) are plotted in Fig. 1. In general, the topography of the NH ice sheets does not vary substantially between different reconstructions whereas uncertainties show larger for Antarctica (Abe-Ouchi et al., 2015). Values up to 125 meters in ocean depth variations (Fig. 1a) are estimated, representing deepening of the ocean with time. The largest changes in the oceanic boundaries occurred in the northern hemisphere where the extensive areas covered by ice sheets during the LGM were flooded due to the ice melting (blue areas in Fig. 1b). It is important, therefore, to consider these changes when attempting to simulate the last deglaciation, for example by including a varying ocean surface area and volume."

The following citation is added to *References*:

"Abe-Ouchi, A., Saito, F., Kageyama, M., Braconnot, P., Harrison, S. P., Lambeck, K., Otto-Bliesner, B. L., Peltier, W. R., Tarasov, L., Peterschmitt, J.-Y., and Takahashi, K.: Ice-sheet configuration in the

CMIP5/PMIP3 Last Glacial Maximum experiments, Geosci. Model Dev., 8, 3621-3637, https://doi.org/10.5194/gmd-8-3621-2015, 2015.”

I3 The authors should also mention that there have been already many successful publications on glacial-interglacial simulations cycles from EMIC (A. Ganopolski et al., Nature 529, pages 200–203 (2016)) and from GCM (A. Abe-Ouchi et al., Nature 500, (2013)190. Moreover, the authors should better emphasize what in this context would be the added value of accounting for sea level rise.

We add your suggestions to *1 Introduction*:

“Moreover, some research was carried out by using comprehensive climate and ice-sheet models (Abe-Ouchi et al, 2013) or climate models interactively coupled with a dynamic ice-sheet model for studying the last glacial-interglacial cycles (Bonelli et al., 2009; Heinemann et al., 2014; Ganopolski et al., 2016) and more specifically, the LGM (Ziemen et al., 2014). Still, in standard ESMs, land-sea mask is traditionally treated as fixed.”

Later in the same paragraph:

“In the PMIP4 last deglaciation Core experiment design, the bathymetry and land-sea mask are considered boundary conditions that cannot evolve automatically in the model. Thus, the decision of how often to make manual updates was left to the expert (Ivanovic et al., 2016). However, by varying the bathymetry in small steps, the artificial signals produced by changes in the ocean configuration might be reduced yielding to a more realistic representation of the ocean circulation and its interaction with the other climate components during the last deglaciation.¨

The following citations are added to *References*:

“Abe-Ouchi, A., Saito, F., Kawamura, K., Raymo, M. E., Okuno, J. I., Takahashi, K., and Blatter, H.: Insolation-driven 100,000-year glacial cycles and hysteresis of ice-sheet volume, Nature, 500, 190-194, 2013.

Ganopolski, A., Winkelmann, R., Schellnhuber, H. J.: Critical insolation–CO2 relation for diagnosing past and future glacial inception. Nature, 529 (7585): 200 DOI:10.1038/nature16494, 2016.”

I4 Superimposed to the vertical resolution of MPIO, an important issue to be discussed is the choice of the initial horizontal resolution.

We clarify this point in *1 Introduction*:

“In this paper, we use the MPIOM coarse resolution configuration with a curvilinear orthogonal grid (GR30) and two poles (Haak et al., 2003), over Greenland and Antarctica. We decide to use the coarse configuration to reduce the computational time, but the algorithms presented in this paper can easily be adapted to higher resolution grids. In the vertical, the model has 40 unevenly spaced levels, ranging from 15 meters near the surface to several hundred meters in the deep ocean.”

Methodology:

M1 It is not clear for me that accounting for only two big lakes (Caspian and Black Sea), the authors can capture abrupt climate changes occurring during deglaciation, as for instance the 8.2 ka event. Moreover, the evolution of Caspian and Black Sea associated to Eurasian ice-sheet melting and large modification of the catchment is not easy to be reconstructed and depicted. The authors should clarify more explicitly what is the limit of their method. Specifically, they should explain how they cope with river run-off and changes in catchment areas during deglaciation for these two epicontinental seas. These issues have been shown to have drastic consequences on atmosphere and ocean circulation (see for example R. Alkama et al., GRL 33 (21) 2006, R. Alkama et al., 2008, Climate Dynamics. 30 and M. Wary et al, J. Quaternary Sci. 32, 908–922, 2017).

Actually, we are not accounting for lakes in order to capture the abrupt climate changes. Our algorithms are applied within the ocean model and therefore, they work on the ocean domain. In that sense, we are interested only in lakes that are connected to the ocean, that is the Black Sea. The Caspian Sea is, indeed, an exemption because it is not connected to the oceans. However, the Caspian Sea is much larger than the other minor lakes. We decided to include it to solve the SST there that might impact on the climate of Central Asia. Therefore, solving the SST of the Caspian Sea might be important for coupled climate models.

As it was mentioned before, we are presenting a tool that is independent of the uncertainties on the reconstructions. We are not solving the response of the topography to the ice-sheet melting and isostatic adjustments, but we are only prescribing them to our scripts. This is a problem to be accomplished by the ice sheet-solid earth models.

Finally, you are right that changes in catchment areas during deglaciation have drastic consequences on atmosphere and ocean circulation. But, this is a problem that is treated in the hydrologial discharge model (part of the land module) instead of the ocean as described by Riddick et al. (2018), as it is stated in the manuscript.

We clarify these issues at the beginning of section *2 Methodology*:

“Finally, we check for the presence of lakes in the GR30 bathymetry; the Caspian Sea and the Black Sea (under LGM condition, for example) are the only cases that are permitted. Because we are dealing with an ocean model, we are interested in lakes that are connected to the ocean, that is the Black Sea. However, we include the Caspian Sea in our calculations because of its potential impact on the climate of Central Asia. Solving the SST of the Caspian Sea, which is much larger than other minor lakes, might be important for coupled climate simulations. All other lakes need to be removed from the ocean domain either by connecting them to the open ocean or by considering them as land. The atmospheric model component allows accounting for lakes on land (only the thermal component). The adequate place to calculate water storage in lakes is the hydrological discharge model.”

M2 At the end of paragraph 2.3, in the spatial smoothing procedure for SSH, there are also changes in water mass reorganization that lead to spatial variations of the sea level rise during melting as shown for instance in Mitrovica (Nature 2001,...). Is this effect accounted for? If not, the authors should clarify the possible impact of this process.

This issue is not specifically part of our algorithms but of the HR prescribed topography that enters to our scripts as input data. We assume that those effects are accounted for in the prescribed topography

which should already contain the gravitational adjustments. In the fully coupled simulation that we are planning to run, the effects you mention are solved by the ice sheet-solid earth component.

Results:

R1 Whereas this paper is submitted for publication in GMD and devoted to technical and model development aspects, it is difficult to consider the validity of the process only analyzing the stability of the response without any information on the potential climate effect. Indeed, accounting for bathymetry with time steps of 10 years should allow the authors to capture the complex pattern of the deglaciation periods. Nevertheless, due to linear smoothing in time and space, it is unclear to me whether they really may capture abrupt events. This limitation should be discussed in more details.

As it was discussed before, the aim of this paper is to present a tool that allows for automatic changes of bathymetry and land-sea mask in the ocean component of MPI-ESM. We are not attempting here to analyse the climate response to a changing topography. The way in which the inclusion of this tool affects on the deglaciation will be studied in the future. The transient simulation exposed in section 3 has the purpose of testing the algorithms in a long-term run. By testing the algorithm we mean the evaluation of the tool in terms of model stability and conservation of water properties as it is stated at the beginning of section *3 Transient simulation*:

“This section has the aim of testing the above-described tool in a long-term run with MPI-ESM. The purpose is not to analyse the climate response to a changing bathymetry and land-sea mask, this will be discussed in a consecutive paper. The aim of this experiment is evaluating the performance of the tool in terms of model stability and conservation of mass and tracers. This is a necessary step towards a fully coupled simulation.”

Due to the changes in the model domain, the fields of SSH and tracers from the restart file are modified. It is therefore important to maintain the same amount of water and tracers inside the system. The choice of 10-years is not crucial for such an evaluation. Knowing that the algorithms guarantee the conservation of water properties, the tool can be applied more often if necessary. Beside this, we are discussing the abrupt flooding of the Hudson Bay in our algorithm.

R2 Superimposed to ice sheet melting, a major component of the SLR is the ocean thermal expansion during deglaciation. Therefore it should produce a difference between SLR and cumulative fresh water input. In fig. 8, I suggest to plot, superimposed to the black and red curves, the component relative to the changes of the ocean volume associated with the thermal expansion during deglaciation.

Thermal expansion is, indeed, not included in the model. MPIOM, as many other ocean models, uses the incompressibility assumption. As a consequence of this, tracers are conservative relative to volume and not relative to mass and the model conserves volume and not mass. Including the thermal expansion term in an ocean model as MPIOM is not consistent with the model physics because it would imply to give up the incompressibility assumption. In any case, the relative effect of thermal expansion on SSH is small compared with the signal due to the freshwater input. We include it in the model description in section *1 Introduction*:

“MPIOM is a free-surface ocean general circulation model with the hydrostatic and Boussinesq approximations and incompressibility assumption.”

We also include a sentence in section *3 Transient simulation*:

“The difference between both time series was divided by the ocean area in order to obtain the errors in mean sea level (Fig. 8b). They are of the order of 1×10^{-3} cm and within the computational accuracy. Therefore, the changes in ocean volume match the freshwater input indicating that water is being conserved. Note that MPIOM uses the incompressibility equations and therefore, the contribution of the thermal expansion on SSH is not being considered here. The year when the Black Sea is connected to the Mediterranean Sea, around 10.3 ka BP, is an exception for the conservation.”

Finally, we do not see the advantage of showing a plot of the thermal expansion in the paper. In addition, changes in volume and mean salinity make it rather tedious to calculate. Traditionally, in ocean models with the incompressibility assumption, thermal expansion can be calculated by using the volume integral over the density, thus giving a mass. The difference of the calculated masses between 2 time slices, can be converted into a volume change (in a real ocean we can assume that volume changes and mass doesn't). Then, dividing the change in ocean volume by the ocean area yield the sea level change by thermal expansion (as was done e.g. in Mikolajewicz et al. 1990). However, here we have the problem that the volume within the ocean model is no longer constant, but the changes are substantial. Therefore, we would have to feed in further assumptions how the additional water entering the ocean should affect the reference mass used for calculation of thermal expansion. As changes in volume are quite large (more than 100 meters in sea level during our simulation) and much larger than the expected value of the thermal expansion (probably a few meters), we would expect quite some uncertainty in the estimation of thermal expansion because of the assumption how to deal with the extra water for the calculation of the reference value. This issue would require a discussion about circulation and climate changes in our deglacial simulation, which is not the topic of this paper.

R3 is the model accounting for a possible ice shelf at the beginning of the deglaciation in the northern hemisphere?

No, MPIOM does not include ice shelves. Therefore, the transient simulation we present does not account for ice shelves in any moment of the run. We include it in the model description in section *1 Introduction*:

“MPIOM includes an embedded dynamic/thermodynamic sea-ice model (Notz et al., 2013) with a viscous-plastic rheology following Hibler (1979). Sea-ice is swimming in the water. Ice shelves are not included. In this paper, we use the MPIOM coarse resolution configuration with a curvilinear orthogonal grid (GR30) and two poles (Haak et al., 2003), over Greenland and Antarctica.”

Remarks:

RM1 As the impact on climate due to change in bathymetry is not described in this paper, we can still have in mind many questions concerning the limits of this tool, when applied to non linear processes as those occurring during deglaciation. Indeed, the deglaciation is far to be a linear process. Major abrupt events (MWP and HE) occurred that are associated with large increase of fresh water inputs. It would be interesting that the authors discuss these potential limitations.

This issue, as already explained before, is not a limitation of our tool but of the prescribed topography and freshwater forcing. We are not solving the topography response to abrupt events, actually. The changes in topography associated with the large increase of freshwater inputs should be included in the

forcing we are prescribing and our algorithms do not depend on it. This would be a task for either the reconstructions or the ice-sheet model, and not for the ocean model. In the fully coupled model under development this will be a very interesting aspect and the model should be suitable to cope with it.

Final comment:
This study is interesting and novel. Moreover, it corresponds to an awaited development to better simulate the last transient deglaciation. Therefore when the authors will have answered the questions raised above, the manuscript will be worth to be published.